Unmanned Systems, Vol. 14, No. 1 (2026) 43–61

DOI: 10.1142/S2301385025500815

UNMANNED SYSTEMS
https://www.worldscientific.com/worldscinet/us

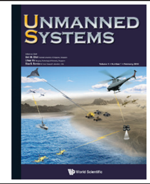

Observer-Based Event-Triggered Fuzzy Control for Switched Multi-Agent Systems with State Constraints and Sensor Faults

Zhen Duan, Hui Yu*

Three Gorges Mathematical Research Center,
China Three Gorges University,
Yichang 443002, P. R. China

College of Science,
China Three Gorges University,
Yichang 443002, P. R. China

In this paper, we consider the output feedback event-triggered tracking control problem for a class of switched nonlinear multi-agent systems (MASs) with sensor faults and state constraints. For unknown nonlinear functions in the system, fuzzy logic systems are used to approximate them. To address sensor faults, sensor error compensation coefficients are designed to compensate for the errors caused by sensor faults. Meanwhile, state observer is designed to estimate the unmeasurable states in the system, providing necessary information for control design. Based on directed switching networks containing a directed spanning tree, an event-triggered output feedback controller is designed to enable the MAS to track the leader agent. By constructing a suitable barrier Lyapunov function, the stability of the system is analyzed, and it is proved that the consensus tracking can be achieved without violating the state constraints, the uniform boundedness of all the closed-loop system signals is ensured and the Zeno behavior can be eliminated. Finally, the effectiveness of the proposed algorithm is verified through a simulation example.

Keywords: Multi-agent systems; sensor faults; event-triggered controller; fuzzy logic system.

1. Introduction

Multi-agent systems (MASs) are composed of a group of interacting agents. Through communication and coordination, all agents can complete a complex task that cannot be completed by a single agent. MASs are ubiquitous in nature and industry, for example, flocks of flying geese, busy and moving ant colonies and cooperative operation of robots [1], smart grid voltage control [2] and so on. Due to the great potential of MASs in applications, numerous scholars have conducted a lot of in-depth research on MASs [3, 4]. The consensus problem of MASs [5, 6] is undoubtedly one of the key research topics. It means that each agent in the system adjusts and updates its behavior via local cooperation and local information exchange, such that all agents can finally reach the same value. Specific applications in practice included unmanned aerial vehicle secure tracking control [7], vehicle-road collaboration [8], etc.

Switched nonlinear system is a system composed of several nonlinear subsystems, and these subsystems can switch according to certain rules or conditions. In practice, such systems are widely found in many fields such as power systems, robot control, and traffic management systems. Therefore, the study of switching nonlinear systems has important theoretical and practical significance. Recently, switched nonlinear MASs have been studied by many researchers [9–12]. In [9], a class of second-order heterogeneous switched nonlinear MASs was studied. The authors proposed an adaptive control strategy based on neural networks to achieve practical finite-time consensus. The consensus problem for a class of heterogeneous

Received 1 July 2024; Accepted 29 September 2024; Published 7 November 2024. This paper was recommended for publication in its revised form by editorial board member, Lu Liu.
Email Address: *yuhui@ctgu.edu.cn*
*Corresponding author.

switched nonlinear MASs was proposed in [10], in which the effects of both cooperative and competitive interactions were considered. In [11], the problem of distributed fault-tolerant consensus tracking for a class of switched nonlinear MASs was studied. The consensus problem for a class of switched nonlinear MASs under cyber-attacks was studied in [12].

Due to the limitations of hardware, the states of the systems may need to be constrained within a certain range. However, the previous works on switched nonlinear MASs did not consider the case of systems with state constraints, which is a very valuable problem in practice. In [13], the fast finite-time consensus algorithm for a class of high-order uncertain nonlinear nonstrict feedback MASs with time-varying asymmetric full-state constraints was considered. An adaptive output feedback quantization consensus control strategy for a class of high-order nonlinear MASs with full state constraints and input lags was studied in [14]. In [15], the problem of distributed adaptive fault-tolerant control for impulsive time-delay nonlinear MASs with state constraints was addressed. A finite-time tracking control method was proposed in [16] for a class of uncertain nonlinear MASs with full state constraints and actuator faults.

Compared with the traditional time-triggered control (TTC) strategy, the event-triggered control (ETC) strategy has great advantages for network systems with limited communication resources. Therefore, the study of ETC strategies for nonlinear MASs is a very active research area. The ETC problem of a class of nonlinear leader-following MASs was proposed in [17]. In [18], an attack-resistant secure ETC scheme was proposed for a class of nonlinear MASs with quantized inputs. The consensus tracking problem for a class of continuously switched stochastic nonlinear MASs was investigated employing ETC strategies in [19]. An ETC approach for nonlinear MASs with Markov switching topology was proposed in [20]. The ETC problem for nonlinear MASs was extensively and deeply studied in [21–25]. Furthermore, it is important to exclude the Zeno behavior in the ETC scheme, that is, the controller does not perform an infinite sampling process in a finite time interval.

In practice, some uncertain factors often exist in nonlinear systems. These uncertainties cannot generally be described by an accurate mathematical model. The fuzzy control strategy based on a fuzzy logic system (FLS) is often used to deal with the uncertainties encountered in practical systems. In [26], the finite-time containment control problem for nonlinear MASs with unavailable states and time delays was studied, in which the FLS was used to approximate the unknown nonlinear functions. In [27], a distributed fuzzy control method was proposed to address the issue of fault-tolerant and timed cooperative control for nonstrict feedback nonlinear MASs with error constraints and input saturation. When the directed communication topology switches and the system's nonlinearity is completely unknown, a distributed fuzzy control method was proposed for MASs to achieve consensus [28]. More results on fuzzy consensus control for MASs can be found in [29–32].

All the research results given in the above literature are based on the normal operation of the system sensors. However, when the sensors in the systems fail, the above control strategies will no longer be applicable. Therefore, in the case of unknown sensor faults, how to ensure the continuous and effective operation of the system has become an important and valuable research topic. In [33], the problem of neural network-based decentralized adaptive sensor fault compensation control was studied for nonlinear switched large-scale systems. The consensus problem of a class of uncertain switched nonlinear MASs with unknown parameters and sensor spoofing attacks was investigated in [34]. In [35], the authors addressed the issue of leader-following consensus control for nonlinear MASs with faulty sensors and actuators under a fixed directed graph. In [36], an adaptive neural network ETC scheme was proposed for nonlinear nonstrict feedback MASs with input saturation, unknown disturbances, and sensor faults. In [37], an adaptive fuzzy consensus tracking control scheme was explored for second-order nonlinear MASs with unmodeled dynamics, external disturbances, and unknown faults in both sensors and actuators.

From the above discussion, it can be seen that although the consensus problem of nonlinear MASs under sensor faults has been widely and deeply studied, but the observer-based event-triggered fuzzy control problem of switched nonlinear MASs with state constraints and unknown sensor faults still deserves further study. The main contributions of this paper are summarized as follows:

(1) By introducing adaptive fault compensation coefficients, a sensor fault compensation control scheme is designed for switched nonlinear MASs. Although the relevant control schemes for switched nonlinear MASs were studied in [9–12], they did not consider the case of systems with sensor faults.
(2) For switched nonlinear MASs, an adaptive event-triggered fuzzy controller is designed, in which the unmeasurable states are estimated by the designed observer through output feedback. It is proved that the proposed event-triggered mechanism will not cause Zeno behavior. Compared with [17–25, 38], the ETC scheme proposed in this paper can be applied to switched nonlinear MASs and save communication resources.
(3) Compared with [13–16], this paper considers the tracking control problem of switched nonlinear MASs

with full state constraints and sensor faults, which is more suitable for practical application.

The rest of this paper is arranged as follows. In Sec. 2, the preliminaries and problem statements are given. The main results are presented in Sec. 3. Section 4 shows the simulation results. Section 5 summarizes the research results of this paper.

2. Problem Statement

2.1. *Graph theory*

To model the communication networks of MASs, a directed graph $\mathcal{G} = (\mathcal{V}, \mathcal{E}, \mathcal{A})$ is used to describe the interconnected relationship between agents, where $\mathcal{V} = \{1, 2, \ldots, N\}$ represents the set of nodes corresponding to N agents, $\mathcal{E} = \mathcal{V} \times \mathcal{V}$ represents the set of edges, and $\mathcal{A} = [a_{ij}] \in R^{N\times N}$ represents the weighted adjacency matrix. If agent i can receive information from agent j, then $(j, i) \in \mathcal{E}$ and $a_{ij} > 0$, else $a_{ij} = 0$. Let $\mathcal{D} = \mathrm{diag}\{d_1, d_2, \ldots, d_n\}$ with $d_i = \sum_{j=1,j\neq i}^{N} a_{ij}$ and the Laplacian matrix is defined as $\mathcal{L} = \mathcal{D} - \mathcal{A}$. Let $\bar{\mathcal{G}}$ be a directed graph with nodes set $\{0, 1, 2, \ldots, N\}$, where the leader agent is labeled as zero. If the agent i can sense the leader's signal, then $a_{i0} > 0$, else $a_{i0} = 0$, and let $\mathcal{B} = \mathrm{diag}(a_{10}, a_{20}, \ldots, a_{N0})$. Starting from the root node, the graph $\bar{\mathcal{G}}$ contains a directed spanning tree if there exists at least one directed path to all the other nodes.

Assumption 2.1. A directed spanning tree rooted at the leader is contained in the directed graph $\bar{\mathcal{G}}$.

Lemma 2.2 ([39]). *Under Assumption* 2.1*, all eigenvalues of the matrix $\mathcal{L} + \mathcal{B}$ have positive real parts.*

2.2. *Problem description*

Consider switched nonlinear MASs consisting of N agents described by

$$\begin{cases} \dot{x}_{ip} = x_{i,p+1} + g_{ip}^{\sigma}(\underline{x}_{ip}) + d_{ip}^{\sigma}, \\ \dot{x}_{in} = u_i + g_{in}^{\sigma}(\underline{x}_{in}) + d_{in}^{\sigma}, \\ y_i = x_{i1}, \quad p = 1, 2, \ldots, n-1, \ i = 1, 2, \ldots, N, \end{cases} \tag{1}$$

and a leader given as $y_r(t)$, where $\sigma(t)$ stands for a switching signal, defined as $\sigma(t) : [0, \infty) \to \mathcal{M} = \{1, 2, \ldots, M\}$ with M being the number of subsystems. x_{ip}, $p = 1, 2, \ldots, n$ represents the pth state of the ith agent. Assume that all states of the system are constrained by the boundary functions $\tau_{c_{ip}}(t)$ and $\tau_{c_{ip}}(t)$, that is, $|x_{ip}| < \tau_{c_{ip}}(t)$ and $|x_{in}| < \tau_{c_{in}}(t)$. Let $\underline{x}_{in} = [x_{i1}, x_{i2}, \ldots, x_{in}]^T$ be the full state. $g_{ip}^{\sigma}(\underline{x}_{ip})$ is a smooth unknown nonlinear function and d_{ip}^{σ} is the bounded unknown external disturbance satisfying $d_{ip}^{\sigma} \leq \bar{d}_{ip}$ with $\bar{d}_{ip}$ being a positive constant. $u_i \in R^n$ is the control input and $y_i \in R^n$ is the system output.

Remark 2.3. Based on the linear system theory, if a general linear system $\dot{x} = Ax + Bu$ is controllable, then it can be transformed into the Brunovsky controller form, which is the linear part of system (1). As an extension of the classical linear system, the nonlinear switching system (1) can be applied to a large class of practical systems, such as, multi-robots, unmanned aerial vehicles, etc.

In this paper, unknown sensor faults occurring at the outputs are considered. For the ith agent, let t_i^F be the moment when the sensor fault occurs and y_i^F is the measured value after the occurrence of a sensor fault after t_i^F. Then, the actual output value can be expressed as follows:

$$y_i^F(t) = \iota_i y_i(t), \quad 0 < \iota_i \leq 1, \ \forall t > t_i^F, \tag{2}$$

where ι_i is the unknown fault factor of the ith agent.

Assumption 2.4. There exists a constant $\underline{\iota}_i$ such that $0 < \underline{\iota}_i \leq \iota_i$.

Remark 2.5. Assumption 2.4 is reasonable. If $\iota_i = 0$, then no feedback information can be obtained, which will cause the system to become uncontrollable. Similar assumptions can be found in [40, 41].

Assumption 2.6. The nth derivative of $y_r(t)$ exists and is bounded.

Lemma 2.7 ([42]). *Let $\tilde{G}(\xi)$ be a continuous function on a compact set Ω_ξ. For any $\zeta > 0$, there exists an FLS $y(\xi) = \tilde{h}^T R(\xi)$ such that*

$$\sup_{\xi\in\Omega_\xi} |\tilde{G}(\xi) - \tilde{h}^T R(\xi)| \leq \zeta,$$

where $y(\xi)$ is the output of the FLS and $\xi = [\xi_1, \xi_2, \ldots, \xi_n]^T$ is the input, $\tilde{h} = [\tilde{h}_1, \tilde{h}_2, \ldots, \tilde{h}_L]^T$ is the weight vector with L being the rule numbers, $R(\xi) = [R_1(\xi), R_2(\xi), \ldots, R_L(\xi)]^T$ is the basis function vector with

$$R_l = \Pi_{i=1}^{n} \mu_{F_i^l}(\xi_i) / \Sigma_{l=1}^{L} (\Pi_{i=1}^{n} \mu_{F_i^l}(\xi_i)),$$

$l = 1, 2, \ldots, L$, and $\mu_{F_i^l}(\xi_i)$ is the fuzzy membership function usually chosen as the Gaussian-type function.

For an uncertain smooth nonlinear function $\tilde{G}(\xi)$, from Lemma 2.7, let $h = \arg\min\{\sup_{\xi\in\Omega_\xi} |\tilde{G}(\xi) - \tilde{h}^T R(\xi)|\}$ be the optimal parameter vector, then one gets

$$\tilde{G}(\xi) = h^T R(\xi) + \zeta(\xi), \tag{3}$$

where $\zeta(\xi)$ is the approximation error satisfying $|\zeta(\xi)| \leq \bar{\zeta}$ with $\bar{\zeta}$ being a positive constant.

Lemma 2.8 ([43]). *For any $\alpha \in R$ and $\forall \delta > 0$, one has*

$$-\alpha \tanh\left(\frac{\alpha}{\delta}\right) \le 0$$

and

$$0 \le |\alpha| - \alpha \tanh\left(\frac{\alpha}{\delta}\right) \le 0.2785\delta.$$

Lemma 2.9 (Young's Inequality, [44]). *For any real number $\alpha \ge 0$ and $\beta \ge 0$,*

$$\alpha\beta \le \frac{\alpha^p}{p} + \frac{\beta^q}{q},$$

where $p > 1$, $q > 1$, and $\frac{1}{p} + \frac{1}{q} = 1$.

Lemma 2.10 ([45]). *For given function $k(t) > 0$, and $e(t)$ satisfy $|e(t)| < k(t)$, we have*

$$\log \frac{k^2(t)}{k^2(t) - e^2(t)} < \frac{e^2(t)}{k^2(t) - e^2(t)}.$$

Lemma 2.11 ([46]). *The cubic absolute-value function $V_x = \frac{1}{3}|x(t)|^3$ is differentiable, and its time derivative is $\dot{V}_x = x^2\dot{x}\mathrm{sign}(x)$.*

The main objectives of this paper are to design an observer-based event-triggered fuzzy control strategy for switched nonlinear MASs with sensor faults, so that the system can track the leader signal y_r, all states in the closed-loop system are uniformly bounded, and state constraints are not violated. In addition, the Zeno phenomenon can be excluded successfully.

3. Control Design

3.1. *State observer design*

The state observer under sensor fault is constructed as follows

$$\begin{cases} \dot{\hat{x}}_{ip} = \hat{x}_{i,p+1} + l_{ip}(\hat{\varpi}_i y_i^F - \hat{y}_i), \\ \dot{\hat{x}}_{in} = u_i + l_{in}(\hat{\varpi}_i y_i^F - \hat{y}_i), \\ \hat{y}_i = \hat{x}_{i1}, \end{cases} \tag{4}$$

where $\hat{x}_{ip}$, $\hat{x}_{in}$ are states of the observer, $\hat{y}_i$ is the output of the observer, $\hat{\varpi}_i$ is the estimation of ϖ_i with $\varpi_i = \frac{1}{\iota_i}$, and $\tilde{\varpi}_i = \varpi_i - \hat{\varpi}_i$.

Let $x_i = [x_{i1}, x_{i2}, \ldots, x_{in}]^T$, $\hat{x}_i = [\hat{x}_{i1}, \hat{x}_{i2}, \ldots, \hat{x}_{in}]^T$, $d_i^\sigma = [d_{i1}^\sigma, d_{i2}^\sigma, \ldots, d_{in}^\sigma]$ and $\tilde{x}_i = x_i - \hat{x}_i$.

From (4), we have

$$\dot{\tilde{x}}_i = A_i\tilde{x}_i + G_i^\sigma + d_i^\delta + L_i\tilde{\varpi}_i y_i^F, \tag{5}$$

where $G_i^\sigma = [g_{i1}^\sigma, g_{i2}^\sigma, \ldots, g_{in}^\sigma]^T$,

$$A_i = \begin{pmatrix} -l_{i1} & 1 & \ldots & 0 \\ -l_{i2} & \vdots & \ddots & \vdots \\ \vdots & 0 & \ldots & 1 \\ -l_{in} & 0 & \ldots & 0 \end{pmatrix},$$

$L_i = [l_{i1}, l_{i2}, \ldots, l_{in}]^T$ is a design parameter vector such that the matrix A_i is Hurwirz. Then, for any positive definite matrix Q_i, there exists a positive definite matrix P_i such that $A_i^T P_i + P_i A_i = -2Q_i$.

Remark 3.1. Matrix A_i is Hurwitz (or stable), indicating that all eigenvalues of matrix A_i possess negative real parts. The design parameters $l_{i1}, l_{i2}, \ldots, l_{in}$ are the coefficients of the Hurwitz polynomial $\underline{p}(x) = x^n + l_{i1}x^{n-1} + \cdots + l_{i,n-1}x + l_{in}$. Given n roots of a Hurwitz polynomial with negative real parts, the Hurwitz polynomial coefficients can be obtained by using the MATLAB command *poly*.

The Lyapunov function candidate is designed as

$$V_{i0} = \tilde{x}_i^T P_i \tilde{x}_i \tag{6}$$

and

$$V_0 = \sum_{i=1}^N V_{i0} = \sum_{i=1}^N \tilde{x}_i^T P_i \tilde{x}_i. \tag{7}$$

The time derivative of V_{i0} is

$$\dot{V}_{i0} = 2\tilde{x}_i^T P_i \dot{\tilde{x}}_i = 2\tilde{x}_i^T P_i (A_i\tilde{x}_i + G_i^\sigma + d_i^\sigma + L_i\tilde{\varpi}_i y_i^F). \tag{8}$$

From Lemma 2.7, for the uncertain nonlinear function $g_{ip}^\sigma(\underline{x}_{ip})$, $p = 1, 2, \ldots, n$, there exists an FLS $(\mathcal{H}_{ip}^\sigma)^T \mathcal{R}_{ip}^\sigma(\underline{x}_{ip})$ such that

$$g_{ip}^\sigma(\underline{x}_{ip}) = (\mathcal{H}_{ip}^\sigma)^T \mathcal{R}_{ip}^\sigma(\underline{x}_{ip}) + \zeta_{ip}^\sigma(\underline{x}_{ip}), \tag{9}$$

where ζ_{ip}^σ is the approximate error satisfying $|\zeta_{ip}^\sigma| \le \bar{\zeta}_{ip}^\sigma$ with $\bar{\zeta}_{ip}^\sigma$ being a positive constant.

Denote $\tilde{G}_i^\sigma(\underline{x}_{ip}) = [\mathcal{H}_{i1}^\sigma \mathcal{R}_{i1}^\sigma(\underline{x}_{ip}), \ldots, \mathcal{H}_{in}^\sigma \mathcal{R}_{in}^\sigma(\underline{x}_{ip})]^T$, $\zeta_i^\sigma = [\zeta_{i1}^\sigma, \ldots, \zeta_{in}^\sigma]^T$, $\bar{\zeta}_i^\sigma = [\bar{\zeta}_{i1}^\sigma, \ldots, \bar{\zeta}_{in}^\sigma]^T$, $\mathcal{H}_i^\sigma = [(\mathcal{H}_{i1}^\sigma)^T, \ldots, (\mathcal{H}_{in}^\sigma)^T]^T$, then according to Lemma 4 and (9), we have

$$\begin{aligned} 2\tilde{x}_i^T P_i G_i^\sigma &= 2\tilde{x}_i^T P_i (G_i^\sigma(\underline{x}_{in}) + \zeta_i^\sigma(\underline{x}_{in})) \\ &\le 2\lambda_{\max}^2(P_i)\|x_i\|^2 + \|\tilde{G}_i^\sigma(\underline{x}_{in})\|^2 \\ &\quad + \|\zeta_i^\sigma(\underline{x}_{in})\|^2. \end{aligned} \tag{10}$$

Note that $\|\tilde{G}_i^\sigma(\underline{x}_{ip})\|^2 = \sum_{p=1}^n ((\mathcal{H}_{ip}^\sigma)^T R_{ip}^\sigma(\underline{x}_{ip}))^2$, according to Cauchy–Schwartz inequality, and $0 < (\mathcal{R}_{ip}^\sigma(\underline{x}_{ip}))^T \mathcal{R}_{ip}^\sigma(\underline{x}_{ip}) \le 1$, we have

$$\sum_{p=1}^n ((\mathcal{H}_{ip}^\sigma)^T R_{ip}^\sigma(\underline{x}_{ip}))^2 \le \sum_{p=1}^n \|\mathcal{H}_{ip}^\sigma\|^2 \|R_{ip}^\sigma(\underline{x}_{ip})\|^2$$

$$\leq \sum_{p=1}^{n} \|\mathcal{H}_{ip}^{\sigma}\|^2 = \|\mathcal{H}_i^{\sigma}\|^2. \tag{11}$$

According to (10) and (11), we have

$$\begin{aligned}2\tilde{x}_i^T P_i G_i^{\sigma} &\leq 2\lambda_{\max}^2(P_i)\|\tilde{x}_i\|^2 + \|\mathcal{H}_i^{\sigma}\|^2 + \|\zeta_i^{\sigma}(\underline{x}_{in})\|^2 \\ &\leq 2\lambda_{\max}^2(P_i)\|\tilde{x}_i\|^2 + \bar{\mathcal{H}}_i^2 + \|\bar{\zeta}_i^{\sigma}(\underline{x}_{in})\|^2 \\ &\leq 2\lambda_{\max}^2(P_i)\|\tilde{x}_i\|^2 + \bar{\mathcal{H}}_i^2 + \bar{\zeta}_i^2,\end{aligned} \tag{12}$$

where $\bar{\mathcal{H}}_i = \max_{\sigma\in\mathcal{M}}\{\|\mathcal{H}_i^{\sigma}\|\}$, $\bar{\zeta}_i = \max_{\sigma\in\mathcal{M}}\{\|\bar{\zeta}_i^{\sigma}\|\}$.

$$\begin{aligned}&2\tilde{x}_i^T P_i(A_i\tilde{x}_i + d_i^{\sigma} + L_i\tilde{\varpi}_i y_i^F) \\ &\quad\leq -(\varrho_i - 2\lambda_{\max}^2(P_i))\|\tilde{x}_i\|^2 + \|L_i\|^2(\tilde{\varpi}_i y_i^F)^2 + \bar{d}_i^2,\end{aligned} \tag{13}$$

where $\varrho_i = 2\lambda_{\min}(Q_i)$, $\bar{d}_i = \max_{\sigma\in\mathcal{M}}\{\|d_i^{\sigma}\|\}$.

From (8) to (13), we have

$$\begin{aligned}\dot{V}_{i0} \leq& -(\varrho_i - 4\lambda_{\max}^2(P_i))\|\tilde{x}_i\|^2 + \|L_i\|^2(\tilde{\varpi}_i y_i^F)^2 \\ &+ \bar{\mathcal{H}}_i^2 + \bar{\zeta}_i^2 + \bar{d}_i^2.\end{aligned} \tag{14}$$

Then from (7) and (14), we have

$$\begin{aligned}\dot{V}_0 \leq& \sum_{i=1}^{N}\{-(\varrho_i - 4\lambda_{\max}^2(P_i))\|\tilde{x}_i\|^2 + \|L_i\|^2(\tilde{\varpi}_i y_i^F)^2 \\ &+ M_i\},\end{aligned} \tag{15}$$

where $M_i = \bar{\mathcal{H}}_i^2 + \bar{\zeta}_i^2 + \bar{d}_i^2$.

3.2. *Back stepping controller design*

Perform the following coordinate transformation:

$$\begin{cases} z_{i1} = \sum_{j\in\mathcal{N}_i} a_{ij}(\hat{x}_{i1} - \hat{x}_{j1}) + a_{i0}(\hat{y}_i - y_r), \\ z_{iq} = \hat{x}_{iq} - \alpha_{i,q-1}, \quad q = 2,3,\ldots,n, \end{cases} \tag{16}$$

where $\alpha_{i,q-1}$ is the virtual control signal at step q.

Let $z_1 = [z_{11}, z_{21}, \ldots, z_{N1}]^T$ and $\hat{y} = [\hat{y}_1, \hat{y}_2, \ldots, \hat{y}_N]^T$. According to (16), we have

$$z_1 = (\mathcal{L} + \mathcal{B})(\hat{y} - 1_N y_r), \tag{17}$$

where 1_N is an N-dimensional column vector with components being all ones.

Step 1. The Lyapunov function is chosen as

$$V_{i1} = V_{i0} + \frac{1}{2}\log\frac{\tau_{i1}^2}{\tau_{i1}^2 - z_{i1}^2} + \frac{1}{2\eta_{i1}}\tilde{\theta}_{i1}^2 + \frac{1}{3w_i}|\tilde{\varpi}_i|^3, \tag{18}$$

where η_{i1} and w_i are positive design parameters, $\tau_{i1}(t)$ is a boundary function satisfying $|z_{i1}(t)| < \tau_{i1}(t)$, $\tilde{\theta}_{i1} = \theta_{i1} - \hat{\theta}_{i1}$, with $\hat{\theta}_{i1}$ being the estimation of θ_{i1}, and the definition of θ_{i1} will be given later.

Remark 3.2. Since both V_{i0} and $\tilde{\theta}_{i1}^2$ are quadratic functions, their derivability is obvious. The derivability of $\log\frac{\tau_{i1}^2}{\tau_{i1}^2 - z_{i1}^2}$ and $|\tilde{\varpi}_i|^3$ can be referred to [47] and Lemma 2.11, respectively. Then V_{i1} is differentiable with respect to t.

From (14) and (16) to (18), one obtains that

$$\begin{aligned}\dot{V}_{i1} =& \dot{V}_{i0} + \frac{z_{i1}}{\tau_{i1}^2 - z_{i1}^2}\left(\dot{z}_{i1} - \frac{\dot{\tau}_{i1}}{\tau_{i1}}z_{i1}\right) - \frac{1}{\eta_{i1}}\tilde{\theta}_{i1}\dot{\hat{\theta}}_{i1} \\ &- \frac{1}{w_i}\tilde{\varpi}_i^2\dot{\tilde{\varpi}}_i\mathrm{sign}(\tilde{\varpi}_i) \\ \leq& -(\varrho_i - 4\lambda_{\max}^2(P_i))\|\tilde{x}_i\|^2 + \|L_i\|^2(\tilde{\varpi}_i y_i^F)^2 + M_{i0} \\ &+ \frac{z_{i1}}{\tau_{i1}^2 - z_{i1}^2}\Big[\Delta_i z_{i2} + \Delta_i\alpha_{i1} + \Delta_i l_{i1}(\hat{\varpi}_i y_i^F - \hat{x}_{i1}) \\ &- \sum_{j\in\mathcal{N}_i} a_{ij}(\hat{x}_{j2} + l_{j2}(\varpi_i y_i^F - \hat{x}_{j1})) - a_{i0}\dot{y}_r \\ &- \frac{\dot{\tau}_{i1}}{\tau_{i1}}z_{i1}\Big] - \frac{1}{\eta_{i1}}\tilde{\theta}_{i1}\hat{\theta}_{i1} - \frac{1}{w_i}\tilde{\varpi}_i^2\dot{\tilde{\varpi}}_i\mathrm{sign}(\tilde{\varpi}_i),\end{aligned} \tag{19}$$

where $\Delta_i = \sum_{j\in\mathcal{N}_i} a_{ij} + a_{i0}$ and $\mathrm{sign}(\cdot)$ is the sign function.

By Young's inequality, we have

$$\Delta_i\frac{z_{i1}}{\tau_{i1}^2 - z_{i1}^2}z_{i2} \leq \frac{1}{2}\Delta_i^2\frac{z_{i1}^2}{(\tau_{i1}^2 - z_{i1}^2)^2} + \frac{1}{2}z_{i2}^2. \tag{20}$$

In conjunction with Lemma 2.7, there exist an FLS $(h_{i1}^{\sigma})^T R_{i1}^{\sigma}(\xi_{i1})$ such that

$$\begin{aligned}\tilde{G}_{i1}^{\sigma}(\xi_{i1}) =& \Delta_i l_{i1}(\hat{\varpi}_i y_i^F - \hat{x}_{i1}) + \frac{1}{2}\Delta_i^2\frac{z_{i1}^2}{(\tau_{i1}^2 - z_{i1}^2)^2} \\ &- \sum_{j\in\mathcal{N}_i} a_{ij}[\hat{x}_{j2} + l_{j2}(\varpi_i y_j^F - \hat{x}_{j1})] - a_{i0}\dot{y}_r \\ &- \frac{\dot{\tau}_{i1}}{\tau_{i1}}z_{i1} \\ =& (h_{i1}^{\sigma})^T R_{i1}^{\sigma}(\xi_{i1}) + \zeta_{i1}^{\sigma},\end{aligned} \tag{21}$$

where $\xi_{i1} = [y_r, y_i^F, \hat{x}_{i1}, \hat{x}_{j1}, \hat{x}_{j2}, \hat{\varpi}_i]^T$, and ζ_{i1}^{σ} is the approximation error satisfying $|\zeta_{i1}^{\sigma}| < \bar{\zeta}_{i1}$ with $\bar{\zeta}_{i1}$ being a positive constant.

Substituting (20) and (21) into (19), one has

$$\begin{aligned}\dot{V}_{i1} \leq& -(\varrho_i - 4\lambda_{\max}^2(P_i))\|\tilde{x}_i\|^2 + \|L_i\|^2(\tilde{\varpi}_i y_i^F)^2 + M_{i0} \\ &+ \frac{z_{i1}}{\tau_{i1}^2 - z_{i1}^2}[\Delta_i\alpha_{i1} + (h_{i1}^{\sigma})^T R_{i1}^{\sigma}(\xi_{i1}) + \zeta_{i1}^{\sigma}] + \frac{1}{2}z_{i2}^2 \\ &- \frac{1}{\eta_{i1}}\tilde{\theta}_{i1}\dot{\hat{\theta}}_{i1} - \frac{1}{w_i}\tilde{\varpi}_i^2\dot{\tilde{\varpi}}_i\mathrm{sign}(\tilde{\varpi}_i).\end{aligned} \tag{22}$$

Applying Young's inequality and with the fact that $0 < R_{i1}^{\sigma T}R_{i1}^{\sigma} \leq 1$, it yields that

$$\frac{z_{i1}}{\tau_{i1}^2 - z_{i1}^2}(h_{i1}^{\sigma})^T R_{i1}^{\sigma} \leq \frac{1}{4r_{i1}} + r_{i1}\frac{z_{i1}^2}{(\tau_{i1}^2 - z_{i1}^2)^2}\theta_{i1}, \tag{23}$$

where $r_{i1} > 0$ is a design parameter, and $\theta_{i1} = \max_{\sigma\in\mathcal{M}}\{\|h_{i1}^{\sigma}\|^2\}$.

Similarly,

$$\frac{z_{i1}}{\tau_{i1}^2 - z_{i1}^2}\zeta_{i1}^{\sigma} \leq \frac{1}{2}\frac{z_{i1}^2}{(\tau_{i1}^2 - z_{i1}^2)^2} + \frac{1}{2}\bar{\zeta}_{i1}^2. \tag{24}$$

Design the virtual control law α_{i1} and the adaptive law $\dot{\hat{\theta}}_{i1}$ as

$$\alpha_{i1} = -\frac{k_{i1}}{\Delta_i}z_{i1} - \frac{r_{i1}}{\Delta_i}\frac{z_{i1}^2}{(\tau_{i1}^2 - z_{i1}^2)^2}\hat{\theta}_{i1} \tag{25}$$

and

$$\dot{\hat{\theta}}_{i1} = \eta_{i1}r_{i1}\frac{z_{i1}^2}{(\tau_{i1}^2 - z_{i1}^2)^2} - \eta_{i1}^*\hat{\theta}_{i1}, \tag{26}$$

where k_{i1}, $\eta_{i1}^* > 0$ are design parameters.

In order to compensate the influence of sensor fault, the adaptive update law of the sensor fault compensation factor is designed as

$$\dot{\hat{\varpi}}_i = \begin{cases} 0 & \text{if } \hat{\varpi}_i = 1, \quad \rho \leq 0 \quad \text{or} \quad \hat{\varpi}_i = \frac{1}{\underline{\iota}}, \ \rho \geq 0, \\ \rho & \text{otherwise}, \end{cases} \tag{27}$$

with

$$\rho = \begin{cases} w_i(y_i^F)^2\|L_i\|^2 - w_i^*\hat{\varpi}_i & \text{if } \Xi_i \geq 0, \\ 0 & \text{if } \Xi_i < 0, \end{cases} \tag{28}$$

where $\Xi_i = w_i(y_i^F)^2\|L_i\|^2 - w_i^*\hat{\varpi}_i$ and $w_i^* > 0$ is a design parameter.

Taking (23)–(28) into (22), one gets

$$\dot{V}_{i1} \leq -(\varrho_i - 4\lambda_{\max}^2(P_i))\|\tilde{x}_i\|^2 - k_{i1}\frac{z_{i1}^2}{(\tau_{i1}^2 - z_{i1}^2)^2} + \frac{1}{2}z_{i2}^2 + \frac{\eta_{i1}^*}{\eta_{i1}}\tilde{\theta}_{i1}\hat{\theta}_{i1} + \frac{w_i^*}{w_i}\tilde{\varpi}_i{}^2\hat{\varpi}_i\text{sign}(\tilde{\varpi}_i) + M_{i1}, \tag{29}$$

where $M_{i1} = M_i + \frac{1}{4r_{i1}} + \frac{1}{2}\bar{\zeta}_{i1}^2$.

Let $V_1 = \sum_{i=1}^N V_{i1}$, then

$$\dot{V}_1 \leq \sum_{i=1}^N \left\{ -(\varrho_i - 4\lambda_{\max}^2(P_i))\|\tilde{x}_i\|^2 - k_{i1}\frac{z_{i1}^2}{\tau_{i1}^2 - z_{i1}^2} + \frac{1}{2}z_{i2}^2 + \frac{\eta_{i1}^*}{\eta_{i1}}\tilde{\theta}_{i1}\hat{\theta}_{i1} + \frac{w_i^*}{w_i}\tilde{\varpi}_i{}^2\hat{\varpi}_i\text{sign}(\tilde{\varpi}_i) + M_{i1} \right\}. \tag{30}$$

Step 2. Choose the Lyapunov function V_2 as

$$V_2 = V_1 + \sum_{i=1}^N \left(\frac{1}{2}\log\frac{\tau_{i2}^2}{\tau_{i2}^2 - z_{i2}^2} + \frac{1}{2\eta_{i2}}\tilde{\theta}_{i2}^2 \right), \tag{31}$$

where $\tau_{i2}(t)$ is a boundary function satisfying $|z_{i2}(t)| < \tau_{i2}(t)$, $\tilde{\theta}_{i2} = \theta_{i2} - \hat{\theta}_{i2}$ with $\hat{\theta}_{i2}$ being the estimation of θ_{i2}, and the definition of θ_{i2} will be given later.

Taking the derivative of V_2 with respect to t yields that

$$\dot{V}_2 = \dot{V}_1 + \sum_{i=1}^N \left\{ \frac{z_{i2}}{\tau_{i2}^2 - z_{i2}^2}\left(\dot{z}_{i2} - \frac{\dot{\tau}_{i2}}{\tau_{i2}}z_{i2} \right) - \frac{1}{\eta_{i2}}\tilde{\theta}_{i2}\dot{\hat{\theta}}_{i2} \right\}. \tag{32}$$

Note that

$$\dot{z}_{i2} = z_{i3} + \alpha_{i2} + l_{i2}(\hat{\varpi}_i y_i^F - \hat{x}_{i1}) - \dot{\alpha}_{i1}. \tag{33}$$

By Young's inequality, one obtains that

$$\frac{z_{i2}}{\tau_{i2}^2 - z_{i2}^2}z_{i3} \leq \frac{z_{i2}^2}{(\tau_{i2}^2 - z_{i2}^2)^2} + \frac{1}{2}z_{i3}^2 \tag{34}$$

and

$$\dot{\alpha}_{i1} = \frac{\partial\alpha_{i1}}{\partial\hat{x}_{i1}}\dot{\hat{x}}_{i1} + \frac{\partial\alpha_{j1}}{\partial\hat{x}_{j1}}\dot{\hat{x}}_{j1} + \frac{\partial\alpha_{i1}}{\partial y_r}\dot{y}_r + \frac{\partial\alpha_{i1}}{\partial\dot{y}_r}\ddot{y}_r + \frac{\partial\alpha_{i1}}{\partial y_i^F}\dot{y}_i^F + \frac{\partial\alpha_{i1}}{\partial\hat{\varpi}_i}\dot{\hat{\varpi}}_i + \frac{\partial\alpha_{i1}}{\partial\hat{\theta}_{i1}}\dot{\hat{\theta}}_{i1} + \frac{\partial\alpha_{i1}}{\partial\tau_{i1}}\dot{\tau}_{i1} + \frac{\partial\alpha_{i1}}{\partial\dot{\tau}_{i1}}\ddot{\tau}_{i1}. \tag{35}$$

Noticing that $0 < \iota_i \leq 1$, one gets that

$$\begin{aligned} &\frac{z_{i2}}{\tau_{i2}^2 - z_{i2}^2}\frac{\partial\alpha_{i1}}{\partial y_i^F}\dot{y}_i^F \\ &= \frac{z_{i2}}{\tau_{i2}^2 - z_{i2}^2}\frac{\partial\alpha_{i1}}{\partial y_i^F}\iota\dot{y}_i \leq \frac{z_{i2}}{\tau_{i2}^2 - z_{i2}^2}\frac{\partial\alpha_{i1}}{\partial y_i^F}\dot{y}_i \\ &= \frac{z_{i2}}{\tau_{i2}^2 - z_{i2}^2}\frac{\partial\alpha_{i1}}{\partial y_i^F}(\hat{x}_{i2} + \tilde{x}_{i2} + g_{i1}^{\sigma} + d_{i1}). \end{aligned} \tag{36}$$

According to Young's inequality, we have

$$\begin{aligned} &\frac{z_{i2}}{\tau_{i2}^2 - z_{i2}^2}\frac{\partial\alpha_{i1}}{\partial y_i^F}(\tilde{x}_{i2} + d_{i1}) \\ &\leq \left(\frac{z_{i2}}{\tau_{i2}^2 - z_{i2}^2}\frac{\partial\alpha_{i1}}{\partial y_i^F} \right)^2 + \frac{1}{2}\|\tilde{x}_i\|^2 + \frac{1}{2}\bar{d}_{i1}^2. \end{aligned} \tag{37}$$

Substituting (37) into (36), one has

$$\begin{aligned} &\frac{z_{i2}}{\tau_{i2}^2 - z_{i2}^2}\frac{\partial\alpha_{i1}}{\partial y_i^F}\dot{y}_i^F \\ &\leq \frac{z_{i2}}{\tau_{i2}^2 - z_{i2}^2}\frac{\partial\alpha_{i1}}{\partial y_i^F}(\hat{x}_{i2} + g_{i1}^{\sigma}) + \left(\frac{z_{i2}}{\tau_{i2}^2 - z_{i2}^2}\frac{\partial\alpha_{i1}}{\partial y_i^F} \right)^2 \\ &\quad + \frac{1}{2}\|\tilde{x}_i\|^2 + \frac{1}{2}\bar{d}_{i1}^2 \end{aligned} \tag{38}$$

and

$$\begin{aligned} &\frac{z_{i2}}{\tau_{i2}^2 - z_{i2}^2}\frac{\partial\alpha_{i1}}{\partial\hat{\varpi}_i}\dot{\hat{\varpi}}_i \\ &\leq \frac{z_{i2}}{\tau_{i2}^2 - z_{i2}^2}\frac{\partial\alpha_{i1}}{\partial\hat{\varpi}_i}(w_i(y_i^F)^2\|L_i\|^2) \\ &\leq \frac{1}{4r_{\varpi_{i1}}} + r_{\varpi_{i1}}\left[\frac{z_{i2}}{\tau_{i2}^2 - z_{i2}^2}\frac{\partial\alpha_{i1}}{\partial\hat{\varpi}_i}(w_i(y_i^F)^2\|L_i\|^2) \right]^2, \end{aligned} \tag{39}$$

where $r_{\varpi_{i1}} > 0$ is a design parameter.

Remark 3.3. Note that the FLS can only approximate a continuous function on a compact set. Because the term $\dot{\hat{\varpi}}_i$ contained in (35) may not be continuous, the virtual controller cannot be placed directly into the FLS. By reducing the inequality (39), a continuous function defined in (40) is obtained.

Let

$$\begin{aligned}\tilde{G}_{i2}(\xi_{i2}) = {}& l_{i2}(\hat{\varpi}_i y_i^F - \hat{x}_{i1}) + \frac{\partial \alpha_{i1}}{\partial \hat{x}_{i1}}\dot{\hat{x}}_{i1} + \frac{\partial \alpha_{i1}}{\partial \hat{x}_{j1}}\dot{\hat{x}}_{j1} + \frac{\partial \alpha_{i1}}{\partial y_r}\dot{y}_r \\ & + \frac{\partial \alpha_{i1}}{\partial \dot{y}_r}\ddot{y}_r + \frac{\partial \alpha_{i1}}{\partial \hat{\theta}_{i1}}\dot{\hat{\theta}}_{i1} + \frac{\partial \alpha_{i1}}{\partial \tau_{i1}}\dot{\tau}_{i1} + \frac{\partial \alpha_{i1}}{\partial \dot{\tau}_{i1}}\ddot{\tau}_{i1} \\ & + \frac{\partial \alpha_{i1}}{\partial y_i^F}(\hat{x}_{i2} + g_{i1}^{\sigma}) + \frac{z_{i2}}{\tau_{i2}^2 - z_{i2}^2}\left(\frac{\partial \alpha_{i1}}{\partial y_i^F}\right)^2 \\ & + \frac{1}{2}z_{i2}^2 + \frac{z_{i2}^2}{(\tau_{i2}^2 - z_{i2}^2)^2} - \frac{\dot{\tau}_{i2}}{\tau_{i2}}\frac{z_{i2}^2}{\tau_{i2}^2 - z_{i2}^2} \\ & + r_{\varpi_{i1}}\frac{z_{i2}}{\tau_{i2}^2 - z_{i2}^2}\left(\frac{\partial \alpha_{i1}}{\partial \hat{\varpi}_i}(w_i(y_i^F)^2\|L_i\|^2)\right)^2, \end{aligned} \tag{40}$$

where $\xi_{i2} = [y_r, \dot{y}_r, \ddot{y}_r, y_i^F, \hat{x}_{i1}, \hat{x}_{i2}, \hat{x}_{j1}, \tau_{i1}, \dot{\tau}_{i1}, \hat{\varpi}_i, \hat{\theta}_{i1}]^T$.

From Lemma 2.7, there exist an FLS $(h_{i2}^{\sigma})^T R_{i2}^{\sigma}(\xi_{i2})$ such that

$$\tilde{G}_{i2}^{\sigma}(\xi_{i2}) = (h_{i2}^{\sigma})^T R_{i2}^{\sigma}(\xi_{i2}) + \zeta_{i2}^{\sigma}, \tag{41}$$

where ζ_{i2}^{σ} is the approximation error satisfying $|\zeta_{i2}^{\sigma}| < \bar{\zeta}_{i2}$ with $\bar{\zeta}_{i2}$ being a positive constant.

From (33) to (41), one obtains that

$$\begin{aligned}\dot{V}_2 \le {}& \dot{V}_1 + \sum_{i=1}^{N}\left\{\frac{z_{i2}}{\tau_{i2}^2 - z_{i2}^2}(\alpha_{i2} + h_{i2}^T R_{i2} + \zeta_{i2}) + \frac{1}{2}z_{i3}^2 \right. \\ & \left. - \frac{1}{\eta_{i2}}\tilde{\theta}_{i2}\dot{\hat{\theta}}_{i2} + M_{i2}\right\}, \end{aligned} \tag{42}$$

where $M_{i2} = \frac{1}{2}\bar{d}_{i1}^2 + \frac{1}{4r_{\varpi_{i1}}}$.

According to Young's inequality and with the fact that $0 < R_{i2}^{\sigma T} R_{i2}^{\sigma} \le 1$, we have

$$\frac{z_{i2}}{\tau_{i2}^2 - z_{i2}^2}(h_{i2}^{\sigma})^T R_{i2}^{\sigma} \le \frac{1}{4r_{i2}} + r_{i2}\frac{z_{i2}^2}{(\tau_{i2}^2 - z_{i2}^2)^2}\theta_{i2}, \tag{43}$$

where $r_{i2} > 0$ is a design parameter and $\theta_{i2} = \max_{\sigma \in \mathcal{M}}\{\|h_{i2}^{\sigma}\|^2\}$.

Similarly,

$$\frac{z_{i2}}{\tau_{i2}^2 - z_{i2}^2}\zeta_{i2}^{\sigma} \le \frac{1}{2}\frac{z_{i2}^2}{(\tau_{i2}^2 - z_{i2}^2)^2} + \frac{1}{2}\bar{\zeta}_{i2}^2. \tag{44}$$

Thus,

$$\begin{aligned}\dot{V}_2 \le {}& \dot{V}_1 + \sum_{i=1}^{N}\left\{\frac{1}{2}z_{i3}^2 + \frac{z_{i2}}{\tau_{i2}^2 - z_{i2}^2}\alpha_{i2} + r_{i2}\frac{z_{i2}^2}{(\tau_{i2}^2 - z_{i2}^2)^2}\theta_{i2} \right. \\ & \left. - \frac{1}{\eta_{i2}}\tilde{\theta}_{i2}\dot{\hat{\theta}}_{i2} + M_{i2}^*\right\}, \end{aligned} \tag{45}$$

where $M_{i2}^* = M_{i2} + \frac{1}{2}\bar{\zeta}_{i2}^2 + \frac{1}{4r_{i2}}$ and $r_{i2} > 0$ is a design parameter.

Design the virtual controller α_{i2} and the adaptive law $\dot{\hat{\theta}}_{i2}$ as

$$\alpha_{i2} = -k_{i2}z_{i2} - r_{i2}\frac{z_{i2}}{\tau_{i2}^2 - z_{i2}^2}\hat{\theta}_{i2} \tag{46}$$

and

$$\dot{\hat{\theta}}_{i2} = \eta_{i2}r_{i2}\frac{z_{i2}^2}{(\tau_{i2}^2 - z_{i2}^2)^2} - \eta_{i2}^*\hat{\theta}_{i2}, \tag{47}$$

where $k_{i2}, \eta_{i2}^* > 0$ are design parameters.

Substituting (30) and (46), (47) into (45), one obtains that

$$\begin{aligned}\dot{V}_2 \le {}& \sum_{i=1}^{N}\left\{-\left(\varrho_i - 4\lambda_{\max}^2(P_i) - \frac{1}{2}\right)\|\tilde{x}_i\|^2 \right. \\ & - k_{i1}\frac{z_{i1}^2}{\tau_{i1}^2 - z_{i1}^2} - k_{i2}\frac{z_{i2}^2}{\tau_{i2}^2 - z_{i2}^2} + \frac{1}{2}z_{i3}^2 + \frac{\eta_{i1}^*}{\eta_{i1}}\tilde{\theta}_{i1}\hat{\theta}_{i1} \\ & \left. + \frac{\eta_{i2}^*}{\eta_{i2}}\tilde{\theta}_{i2}\hat{\theta}_{i2} + \frac{w_i^*}{w_i}\tilde{\varpi}_i{}^2\hat{\varpi}_i\mathrm{sign}(\tilde{\varpi}_i) + \tilde{M}_{i2}\right\}, \end{aligned} \tag{48}$$

where $\tilde{M}_{i2} = M_{i1} + M_{i2}^*$.

Step 3. The Lyapunov function V_3 is chosen as

$$V_3 = V_2 + \sum_{i=1}^{N}\left(\frac{1}{2}\log\frac{\tau_{i3}^2}{\tau_{i3}^2 - z_{i3}^2} + \frac{1}{2\eta_{i3}}\tilde{\theta}_{i3}^2\right), \tag{49}$$

where $\tau_{i3}(t)$ is a boundary function satisfying $|z_{i3}(t)| < \tau_{i3}(t)$, $\tilde{\theta}_{i3} = \theta_{i3} - \hat{\theta}_{i3}$, $\hat{\theta}_{i3}$ is the estimation of θ_{i3}, and the definition of θ_{i3} will be given later.

The derivative of V_3 with respect to t is

$$\begin{aligned}\dot{V}_3 = {}& \dot{V}_2 \\ & + \sum_{i=1}^{N}\left\{\frac{z_{i3}}{\tau_{i3}^2 - z_{i3}^2}\left(\dot{z}_{i3} - \frac{\dot{\tau}_{i3}}{\tau_{i3}}z_{i3}\right) - \frac{1}{\eta_{i3}}\tilde{\theta}_{i3}\dot{\hat{\theta}}_{i3}\right\}. \end{aligned} \tag{50}$$

Note that

$$\dot{z}_{i3} = z_{i4} + \alpha_{i3} + l_{i3}(\hat{\varpi}_i y_i^F - \hat{x}_{i1}) - \dot{\alpha}_{i2}. \tag{51}$$

By Young's inequality, one has

$$\frac{z_{i3}}{\tau_{i3}^2 - z_{i3}^2}z_{i4} \le \frac{z_{i3}^2}{(\tau_{i3}^2 - z_{i3}^2)^2} + \frac{1}{2}z_{i4}^2 \tag{52}$$

and

$$\begin{aligned}\dot{\alpha}_{i2} = {}& \frac{\partial \alpha_{i2}}{\partial \hat{x}_{i1}}\dot{\hat{x}}_{i1} + \frac{\partial \alpha_{i2}}{\partial \hat{x}_{i2}}\dot{\hat{x}}_{i2} + \frac{\partial \alpha_{i2}}{\partial \hat{x}_{j1}}\dot{\hat{x}}_{j1} + \frac{\partial \alpha_{i2}}{\partial y_r}\dot{y}_r + \frac{\partial \alpha_{i2}}{\partial \dot{y}_r}\ddot{y}_r \\ & + \frac{\partial \alpha_{i2}}{\partial y_i^F}\dot{y}_i^F + \frac{\partial \alpha_{i2}}{\partial \tau_{i1}}\dot{\tau}_{i1} + \frac{\partial \alpha_{i2}}{\partial \dot{\tau}_{i1}}\ddot{\tau}_{i1} + \frac{\partial \alpha_{i2}}{\partial \tau_{i2}}\dot{\tau}_{i2} + \frac{\partial \alpha_{i2}}{\partial \dot{\tau}_{i2}}\ddot{\tau}_{i2} \\ & + \frac{\partial \alpha_{i2}}{\partial \hat{\varpi}_i}\dot{\hat{\varpi}}_i + \frac{\partial \alpha_{i2}}{\partial \hat{\theta}_{i1}}\dot{\hat{\theta}}_{i1} + \frac{\partial \alpha_{i2}}{\partial \hat{\theta}_{i2}}\dot{\hat{\theta}}_{i2}. \end{aligned} \tag{53}$$

Similar to Step 2, we have

$$\begin{aligned}
&\frac{z_{i3}}{\tau_{i3}^2 - z_{i3}^2}\frac{\partial \alpha_{i2}}{\partial y_i^F}\dot{y}_i^F \\
&= \frac{z_{i3}}{\tau_{i3}^2 - z_{i3}^2}\frac{\partial \alpha_{i2}}{\partial y_i^F}\iota_i\dot{y}_i \\
&\le \frac{z_{i3}}{\tau_{i3}^2 - z_{i3}^2}\frac{\partial \alpha_{i2}}{\partial y_i^F}\dot{y}_i \\
&= \frac{z_{i3}}{\tau_{i3}^2 - z_{i3}^2}\frac{\partial \alpha_{i2}}{\partial y_i^F}(\hat{x}_{i2} + \tilde{x}_{i2} + g_{i1}^\sigma + d_{i1}) \\
&\le \frac{z_{i3}}{\tau_{i3}^2 - z_{i3}^2}\frac{\partial \alpha_{i2}}{\partial y_i^F}(\hat{x}_{i2} + g_{i1}^\sigma) + \left(\frac{z_{i3}}{\tau_{i3}^2 - z_{i3}^2}\frac{\partial \alpha_{i2}}{\partial y_i^F}\right)^2 \\
&\quad + \frac{1}{2}\|\tilde{x}_i\|^2 + \frac{1}{2}\bar{d}_{i1}^2 \qquad (54)
\end{aligned}$$

and

$$\begin{aligned}
&\frac{z_{i3}}{\tau_{i3}^2 - z_{i3}^2}\frac{\partial \alpha_{i2}}{\partial \hat{\varpi}_i}\dot{\hat{\varpi}}_i \\
&\le \frac{z_{i3}}{\tau_{i3}^2 - z_{i3}^2}\frac{\partial \alpha_{i2}}{\partial \hat{\varpi}_i}(w_i(y_i^F)^2\|L_i\|^2) \\
&\le \frac{1}{4r_{\varpi_{i2}}} + r_{\varpi_{i2}}\left[\frac{z_{i3}}{\tau_{i3}^2 - z_{i3}^2}\frac{\partial \alpha_{i2}}{\partial \hat{\varpi}_i}(w_i(y_i^F)^2\|L_i\|^2)\right]^2, \qquad (55)
\end{aligned}$$

where $r_{\varpi_{i2}} > 0$ is a design parameter.

Let

$$\begin{aligned}
\bar{G}_{i3}^\sigma(\xi_{i3}) &= l_{i3}(\hat{\varpi}_i y_i^F - \hat{x}_{i1}) + \frac{\partial \alpha_{i2}}{\partial \hat{x}_{i1}}\dot{\hat{x}}_{i1} + \frac{\partial \alpha_{i2}}{\partial \hat{x}_{i2}}\dot{\hat{x}}_{i2} + \frac{\partial \alpha_{i2}}{\partial \hat{x}_{j1}}\dot{\hat{x}}_{j1} \\
&\quad + \frac{\partial \alpha_{i2}}{\partial y_r}\dot{y}_r + \frac{\partial \alpha_{i2}}{\partial \dot{y}_r}\ddot{y}_r + \frac{\partial \alpha_{i2}}{\partial \hat{\theta}_{i1}}\dot{\hat{\theta}}_{i1} + \frac{\partial \alpha_{i2}}{\partial \hat{\theta}_{i2}}\dot{\hat{\theta}}_{i2} + \frac{1}{2}z_{i3}^2 \\
&\quad + \frac{z_{i3}^2}{(\tau_{i3}^2 - z_{i3}^2)^2} - \frac{\dot{\tau}_{i3}}{\tau_{i3}}\frac{z_{i3}^2}{\tau_{i3}^2 - z_{i3}^2} + \frac{\partial \alpha_{i2}}{\partial \tau_{i1}}\dot{\tau}_{i1} \\
&\quad + \frac{\partial \alpha_{i2}}{\partial \dot{\tau}_{i1}}\ddot{\tau}_{i1} + \frac{\partial \alpha_{i2}}{\partial \tau_{i2}}\dot{\tau}_{i2} + \frac{\partial \alpha_{i2}}{\partial \dot{\tau}_{i2}}\ddot{\tau}_{i2} \\
&\quad + \frac{\partial \alpha_{i2}}{\partial y_i^F}(\hat{x}_{i2} + g_{i1}^\sigma) + \frac{z_{i3}}{\tau_{i3}^2 - z_{i3}^2}\left(\frac{\partial \alpha_{i2}}{\partial y_i^F}\right)^2 \\
&\quad + r_{\varpi_{i2}}\frac{z_{i3}}{\tau_{i3}^2 - z_{i3}^2}\left(\frac{\partial \alpha_{i2}}{\partial \hat{\varpi}_i}(w_i(y_i^F)^2\|L_i\|^2)\right)^2, \qquad (56)
\end{aligned}$$

where

$$\xi_{i3} = [y_r, \dot{y}_r, \ddot{y}_r, y_i^F, \hat{x}_{i1}, \hat{x}_{i2}, \hat{x}_{j1}, \tau_{i1}, \dot{\tau}_{i1}, \tau_{i2}, \dot{\tau}_{i2}, \hat{\varpi}_i, \hat{\theta}_{i1}, \hat{\theta}_{i2}]^T.$$

Similarly, there exist an FLS $(h_{i2}^\sigma)^T R_{i3}^\sigma(\xi_{i3})$ such that

$$\bar{G}_{i3}^\sigma(\xi_{i3}) = (h_{i3}^\sigma)^T R_{i3}^\sigma(\xi_{i3}) + \zeta_{i3}^\sigma, \qquad (57)$$

where ζ_{i3}^σ is the approximation error satisfying $|\zeta_{i3}^\sigma| < \bar{\zeta}_{i3}$ with $\bar{\zeta}_{i3}$ being a positive constant.

Inserting (51)–(57) into (50), one gets that

$$\begin{aligned}
\dot{V}_3 \le \dot{V}_2 + \sum_{i=1}^N \Bigg\{ &\frac{z_{i3}}{\tau_{i3}^2 - z_{i3}^2}(\alpha_{i3} + h_{i3}^T R_{i3} + \zeta_{i3}) + \frac{1}{2}z_{i4}^2 \\
&- \frac{1}{\eta_{i3}}\tilde{\theta}_{i3}\dot{\hat{\theta}}_{i3} + M_{i3}\Bigg\}, \qquad (58)
\end{aligned}$$

where $M_{i3} = \frac{1}{2}\bar{d}_{i1}^2 + \frac{1}{4r_{\varpi_{i2}}}$.

According to Young's inequality and with the fact that $0 < R_{i3}^{\sigma T} R_{i3}^\sigma \le 1$, we have

$$\frac{z_{i3}}{\tau_{i3}^2 - z_{i3}^2}(h_{i3}^\sigma)^T R_{i3}^\sigma \le \frac{1}{4r_{i3}} + r_{i3}\frac{z_{i3}^2}{(\tau_{i3}^2 - z_{i3}^2)^2}\theta_{i3}, \qquad (59)$$

where $r_{i3} > 0$ is a design parameter, and $\theta_{i3} = \max_{\sigma \in \mathcal{M}}\{\|h_{i3}^\sigma\|^2\}$.

Similarly,

$$\frac{z_{i3}}{\tau_{i3}^2 - z_{i3}^2}\zeta_{i3}^\sigma \le \frac{1}{2}\frac{z_{i3}^2}{(\tau_{i3}^2 - z_{i3}^2)^2} + \frac{1}{2}\bar{\zeta}_{i3}^2. \qquad (60)$$

According to (58)–(60), we have

$$\begin{aligned}
\dot{V}_3 \le \dot{V}_2 + \sum_{i=1}^N \Bigg\{ &\frac{1}{2}z_{i4}^2 + \frac{z_{i3}}{\tau_{i3}^2 - z_{i3}^2}\alpha_{i3} \\
&+ r_{i3}\frac{z_{i3}^2}{(\tau_{i3}^2 - z_{i3}^2)^2}\theta_{i3} - \frac{1}{\eta_{i3}}\tilde{\theta}_{i3}\dot{\hat{\theta}}_{i3} + M_{i3}^*\Bigg\}, \qquad (61)
\end{aligned}$$

where $M_{i3}^* = M_{i3} + \frac{1}{2}\bar{\zeta}_{i3}^2 + \frac{1}{4r_{i3}}$.

Select

$$\alpha_{i3} = -k_{i3}z_{i3} - r_{i3}\frac{z_{i3}}{\tau_{i3}^2 - z_{i3}^2}\hat{\theta}_{i3} \qquad (62)$$

and

$$\dot{\hat{\theta}}_{i3} = r_{i3}\frac{z_{i3}^2}{(\tau_{i3}^2 - z_{i3}^2)^2} - \eta_{i3}^*\hat{\theta}_{i3}, \qquad (63)$$

where $k_{i3}, \eta_{i3}^* > 0$ are design parameters.

Substituting (48) and (62), (63) into (61), one has

$$\begin{aligned}
\dot{V}_3 \le \sum_{i=1}^N \Bigg\{ &-(\varrho_i - 4\lambda_{\max}^2(P_i) - 1)\|\tilde{x}_i\|^2 - k_{i1}\frac{z_{i1}^2}{\tau_{i1}^2 - z_{i1}^2} \\
&- k_{i2}\frac{z_{i2}^2}{\tau_{i2}^2 - z_{i2}^2} - k_{i3}\frac{z_{i3}^2}{\tau_{i3}^2 - z_{i3}^2} + \frac{1}{2}z_{i4}^2 + \frac{\eta_{i1}^*}{\eta_{i1}}\tilde{\theta}_{i1}\hat{\theta}_{i1} \\
&+ \frac{\eta_{i2}^*}{\eta_{i2}}\tilde{\theta}_{i2}\hat{\theta}_{i2} + \frac{\eta_{i3}^*}{\eta_{i3}}\tilde{\theta}_{i3}\hat{\theta}_{i3} + \frac{w_i^*}{w_i}\tilde{\varpi}_i{}^2\hat{\varpi}_i\mathrm{sign}(\tilde{\varpi}_i) + \tilde{M}_{i3}\Bigg\}, \\
&\qquad (64)
\end{aligned}$$

where $\tilde{M}_{i3} = \tilde{M}_{i2} + M_{i3}^*$.

Step Ω $(4 \le \Omega \le n-1)$. Choose the Lyapunov function for Step Ω as

$$V_\Omega = V_{\Omega-1} + \sum_{i=1}^N \left(\frac{1}{2}\log\frac{\tau_{i\Omega}^2}{\tau_{i\Omega}^2 - z_{i\Omega}^2} + \frac{1}{2\eta_{i\Omega}}\tilde{\theta}_{i\Omega}^2\right), \qquad (65)$$

where $\tau_{i\Omega}(t)$ is a boundary function satisfying $|z_{i\Omega}(t)| < \tau_{i\Omega}(t)$, $\tilde{\theta}_{i\Omega} = \theta_{i\Omega} - \hat{\theta}_{i\Omega}$, $\hat{\theta}_{i\Omega}$ is the estimation of $\theta_{i\Omega}$, and the definition of $\theta_{i\Omega}$ will be given later.

Similar to Step 3, the virtual controller $\alpha_{i\Omega}$ and the adaptive law $\dot{\hat{\theta}}_{i\Omega}$ are designed as

$$\alpha_{i\Omega} = -k_{i\Omega} z_{i\Omega} - r_{i\Omega} \frac{z_{i\Omega}}{\tau_{i\Omega}^2 - z_{i\Omega}^2} \hat{\theta}_{i\Omega} \tag{66}$$

and

$$\dot{\hat{\theta}}_{i\Omega} = r_{i\Omega} \frac{z_{i\Omega}^2}{(\tau_{i\Omega}^2 - z_{i\Omega}^2)^2} - \eta_{i\Omega}^* \hat{\theta}_{i\Omega}, \tag{67}$$

where $k_{i\Omega}$, $\eta_{i\Omega}^*$, and $r_{i\Omega}$ are positive design parameters.

From (66), (67) and by Young's inequality, one obtains that

$$\begin{aligned}\dot{V}_\Omega \leq & \sum_{i=1}^{N} \Bigg\{ -\left(\varrho_i - 4\lambda_{\max}^2(P_i) - \frac{\Omega}{2} \right) \|\tilde{x}_i\|^2 \\ & - \sum_{s=1}^{\Omega} k_{is} \frac{z_{is}^2}{\tau_{is}^2 - z_{is}^2} + \frac{1}{2} z_{i,\Omega+1}^2 + \sum_{s=1}^{\Omega} \frac{\eta_{is}^*}{\eta_{is}} \tilde{\theta}_{is} \hat{\theta}_{is} \\ & + \frac{w_i^*}{w_i} \tilde{\varpi}_i{}^2 \hat{\varpi}_i \operatorname{sign}(\tilde{\varpi}_i) + \tilde{M}_{i\Omega} \Bigg\},\end{aligned} \tag{68}$$

where $\tilde{M}_{i\Omega} = \bar{d}_i^2 + \frac{\Omega-1}{2} \bar{d}_{i1}^2 + \sum_{s^*=1}^{\Omega-1} \frac{1}{4r_{\varpi_{is^*}}} + \sum_{s=1}^{\Omega} (\frac{1}{2} \bar{\zeta}_{is} + \frac{1}{4r_{is}})$, $|\zeta_{is}^\sigma| < \bar{\zeta}_{is}$ and $\bar{\zeta}_{is}$ is a positive constant.

Step *n*. The Lyapunov function V_{in} is designed as

$$V_{in} = V_{i,n-1} + \frac{1}{2} \log \frac{\tau_{in}^2}{\tau_{in}^2 - z_{in}^2} + \frac{1}{2\eta_{in}} \tilde{\theta}_{in}^2, \tag{69}$$

where $\eta_{in} > 0$ is a design parameter and $\tilde{\theta}_{in}$ will be defined later.

Taking the time derivative of V_{in} yields that

$$\begin{aligned}\dot{V}_{in} = & \dot{V}_{i,n-1} - \frac{1}{\eta_{in}} \tilde{\theta}_{in} \dot{\hat{\theta}}_{in} + \frac{z_{in}}{\tau_{in}^2 - z_{in}^2} \Bigg[u_i + l_{in}(\hat{\varpi}_i y_i^F \\ & - \hat{x}_{i1}) - \dot{\alpha}_{i,n-1} - \frac{\dot{\tau}_{in}}{\tau_{in}} z_{in} \Bigg],\end{aligned} \tag{70}$$

where

$$\begin{aligned}\dot{\alpha}_{i,n-1} = & \frac{\partial \alpha_{i,n-1}}{\partial \hat{\varpi}_i} \dot{\hat{\varpi}}_i + \frac{\partial \alpha_{i,n-1}}{y_i^F} \dot{y}_i^F + \frac{\partial \alpha_{i,n-1}}{\partial y_r} \dot{y}_r + \frac{\partial \alpha_{i,n-1}}{\partial \dot{y}_r} \ddot{y}_r \\ & + \sum_{\Lambda=1}^{n-1} \Bigg(\frac{\partial \alpha_{i,n-1}}{\partial \hat{x}_{i\Lambda}} \dot{\hat{x}}_{i\Lambda} + \frac{\partial \alpha_{i,n-1}}{\partial \hat{\theta}_{i\Lambda}} \dot{\hat{\theta}}_{i\Lambda} + \frac{\partial \alpha_{i,n-1}}{\partial \tau_{i\Lambda}} \dot{\tau}_{i\Lambda} \\ & + \frac{\partial \alpha_{i,n-1}}{\partial \dot{\tau}_{i\Lambda}} \ddot{\tau}_{i\Lambda} \Bigg),\end{aligned} \tag{71}$$

and $\hat{\theta}_{in}$ will be given later.

Similarly,

$$\begin{aligned}& \frac{z_{in}}{\tau_{in}^2 - z_{in}^2} \frac{\partial \alpha_{i,n-1}}{\partial y_i^F} \dot{y}_i^F \\ & = \frac{z_{in}}{\tau_{in}^2 - z_{in}^2} \frac{\partial \alpha_{i,n-1}}{\partial y_i^F} \iota_i \dot{y}_i \\ & \leq \frac{z_{in}}{\tau_{in}^2 - z_{in}^2} \frac{\partial \alpha_{i,n-1}}{\partial y_i^F} \dot{y}_i \\ & = \frac{z_{in}}{\tau_{in}^2 - z_{in}^2} \frac{\partial \alpha_{i,n-1}}{\partial y_i^F} (\hat{x}_{i2} + \tilde{x}_{i2} + g_{i1}^\sigma + d_{i1}) \\ & \leq \frac{z_{in}}{\tau_{in}^2 - z_{in}^2} \frac{\partial \alpha_{i,n-1}}{\partial y_i^F} (\hat{x}_{i2} + g_{i1}^\sigma) \\ & \quad + \left(\frac{z_{in}}{\tau_{in}^2 - z_{in}^2} \frac{\partial \alpha_{i,n-1}}{\partial y_i^F} \right)^2 \\ & \quad + \frac{1}{2} \|\tilde{x}_i\|^2 + \frac{1}{2} \bar{d}_{i1}^2\end{aligned} \tag{72}$$

and

$$\begin{aligned}& \frac{z_{in}}{\tau_{in}^2 - z_{in}^2} \frac{\partial \alpha_{i,n-1}}{\partial \hat{\varpi}_i} \dot{\hat{\varpi}}_i \\ & \leq \frac{z_{in}}{\tau_{in}^2 - z_{in}^2} \frac{\partial \alpha_{i,n-1}}{\partial \hat{\varpi}_i} (w_i (y_i^F)^2 \|L_i\|^2) \\ & \leq \frac{1}{4r_{\varpi_{i,n-1}}} + r_{\varpi_{i,n-1}} \left[\frac{z_{in}}{\tau_{in}^2 - z_{in}^2} \frac{\partial \alpha_{i,n-1}}{\partial \hat{\varpi}_i} (w_i (y_i^F)^2 \|L_i\|^2) \right]^2,\end{aligned} \tag{73}$$

where $r_{\varpi_{i,n-1}} > 0$ is a design parameter.

Let

$$\begin{aligned}& \tilde{G}_{in}^\sigma(\xi_{in}) \\ & = l_{in}(\hat{\varpi}_i y_i^F - \hat{x}_{i1}) + \frac{\partial \alpha_{i,n-1}}{\partial \hat{x}_{j1}} \dot{\hat{x}}_{j1} + \frac{\partial \alpha_{i,n-1}}{\partial y_r} \dot{y}_r + \frac{\partial \alpha_{i,n-1}}{\partial \dot{y}_r} \ddot{y}_r \\ & \quad + \frac{\partial \alpha_{i,n-1}}{\partial y_i^F} (\hat{x}_{i2} + g_{i1}^\sigma) + \frac{z_{in}}{\tau_{in}^2 - z_{in}^2} \left(\frac{\partial \alpha_{i,n-1}}{\partial y_i^F} \right)^2 \\ & + r_{\varpi_{i,n-1}} \frac{z_{in}}{\tau_{in}^2 - z_{in}^2} \left(\frac{\partial \alpha_{in}}{\partial \hat{\varpi}_i} (w_i (y_i^F)^2 \|L_i\|^2) \right)^2 \\ & \quad - \frac{\dot{\tau}_{in}}{\tau_{in}} \frac{z_{in}^2}{\tau_{in}^2 - z_{in}^2} + \sum_{\Lambda=1}^{n-1} \Bigg(\frac{\partial \alpha_{i,n-1}}{\partial \hat{x}_{i\Lambda}} \dot{\hat{x}}_{i\Lambda} + \frac{\partial \alpha_{i,n-1}}{\partial \hat{\theta}_{i\Lambda}} \dot{\hat{\theta}}_{i\Lambda} \\ & \quad + \frac{\partial \alpha_{i,n-1}}{\partial \tau_{i\Lambda}} \dot{\tau}_{i\Lambda} + \frac{\partial \alpha_{i,n-1}}{\partial \dot{\tau}_{i\Lambda}} \ddot{\tau}_{i\Lambda} \Bigg),\end{aligned} \tag{74}$$

where

$$\begin{aligned}\xi_{i3} = & [y_r, \dot{y}_r, \ddot{y}_r, y_i^F, \hat{x}_{i1}, \ldots, \hat{x}_{in}, \hat{x}_{j1}, \tau_{i1}, \ldots, \tau_{in}, \\ & \dot{\tau}_{i1}, \ldots, \dot{\tau}_{in}, \hat{\varpi}_i, \hat{\theta}_{i1}, \ldots, \hat{\theta}_{in}]^T.\end{aligned}$$

Similarly,

$$\tilde{G}_{in}^\sigma(\xi_{in}) = (h_{in}^\sigma)^T R_{in}^\sigma(\xi_{in}) + \zeta_{in}^\sigma(\xi_{in}), \tag{75}$$

where $\zeta_{in}^\sigma(\xi_{in})$ is the approximate error satisfying $|\zeta_{in}^\sigma(\xi_{in})| \leq \bar{\zeta}_{in}$ with $\bar{\zeta}_{in}$ being a positive constant.

Let

$$V_n = \sum_{i=1}^{N} V_{in}, \tag{76}$$

then from (69) to (75) and with the fact that $0<R_{in}^{\sigma T}R_{in}^{\sigma}\le 1$, we have

$$\begin{aligned}\dot{V}_n \le & \sum_{i=1}^{N}\Bigg\{-\Big(\varrho_i - 4\lambda_{\max}^2(P_i)-\frac{n}{2}\Big)\|\tilde{x}_i\|^2 - \sum_{s=1}^{n-1}k_{is}\frac{z_{is}^2}{\tau_{is}^2-z_{is}^2} \\ & + \sum_{s=1}^{n-1}\frac{\eta_{is}^*}{\eta_{is}}\tilde{\theta}_{is}\hat{\theta}_{is} + \frac{w_i^*}{w_i}\varpi_i{}^2\varpi_i \mathrm{sign}(\tilde{\varpi}_i) \\ & + \frac{z_{in}}{\tau_{in}^2-z_{in}^2}(u_i + h_{in}^T R_{in} + \zeta_{in}^{\sigma}) - \frac{1}{\eta_{in}}\tilde{\theta}_{in}\dot{\hat{\theta}}_{in} + M_{in}\Bigg\} \\ \le & \sum_{i=1}^{N}\Bigg\{-\Big(\varrho_i - 4\lambda_{\max}^2(P_i)-\frac{n}{2}\Big)\|\tilde{x}_i\|^2 - \sum_{s=1}^{n-1}k_{is}\frac{z_{is}^2}{\tau_{is}^2-z_{is}^2} \\ & + \sum_{s=1}^{n-1}\frac{\eta_{is}^*}{\eta_{is}}\tilde{\theta}_{is}\hat{\theta}_{is} + \frac{w_i^*}{w_i}\varpi_i{}^2\varpi_i \mathrm{sign}(\tilde{\varpi}_i) + \frac{z_{in}}{\tau_{in}^2-z_{in}^2}u_i \\ & + \frac{1}{2}\frac{z_{in}^2}{(\tau_{in}^2-z_{in}^2)^2} + r_{in}\frac{z_{in}^2}{(\tau_{in}^2-z_{in}^2)^2}\theta_{in} \\ & - \frac{1}{\eta_{in}}\tilde{\theta}_{in}\dot{\hat{\theta}}_{in} + M_{in}\Bigg\}, \end{aligned} \tag{77}$$

where $\theta_{in} = \max_{\sigma\in\mathcal{M}}\{\|h_{in}^{\sigma}\|^2\}$ and $M_{in} = \tilde{M}_{i,n-1} + \frac{1}{2}\bar{d}_{i1}^2 + \frac{1}{4r_{\varpi_{i,n-1}}} + \frac{1}{2}\bar{\zeta}_{in}^2 + \frac{1}{4r_{in}}$.

Design the virtual control law α_{in} and the adaptive law $\dot{\hat{\theta}}_{in}$ as

$$\alpha_{in} = k_{in}z_{in} + \frac{z_{in}}{2(\tau_{in}^2-z_{in}^2)} + r_{in}\frac{z_{in}}{\tau_{in}^2-z_{in}^2}\hat{\theta}_{in} \tag{78}$$

and

$$\dot{\hat{\theta}}_{in} = \eta_{in}r_{in}\frac{z_{in}^2}{(\tau_{in}^2-z_{in}^2)^2} - \eta_{in}^*\hat{\theta}_{in}, \tag{79}$$

where ε_i, k_{in} and η_{in}^* are positive design parameters.

3.3. *Event-triggered controller design*

Design the event-triggered controller as

$$u_i(t) = v_i(t_{ik}), \quad \forall t\in[t_{ik}, t_{i,k+1}), \tag{80}$$

where t_{ik}, $k=0,1,2,\ldots$, is the update moment of event-triggered controller for agent i, and the initial time is denoted by $t_{i0}=t_0$, $t_0\ge 0$.

The control function $v_i(t)$ is designed as

$$\begin{aligned} v_i(t) = & -(1+\gamma_i)\Bigg[\alpha_{in}\tanh\left(\frac{1}{\delta_i}\frac{z_{in}\alpha_{in}}{\tau_{in}^2-z_{in}^2}\right) \\ & + \frac{\varepsilon_i}{1-\gamma_i}\tanh\left(\frac{1}{\delta_i(1-\gamma_i)}\frac{z_{in}\varepsilon_i}{\tau_{in}^2-z_{in}^2}\right)\Bigg], \end{aligned} \tag{81}$$

where $0<\gamma_i<1$ and δ_i is a positive constant.

Let

$$e_i(t) = v_i(t) - u_i(t). \tag{82}$$

The trigger condition is designed as

$$t_{i,k+1} = \inf\{t > t_{ik} \,|\, |e_i(t)| \ge \gamma_i|u_i(t)| + \varepsilon_i\}. \tag{83}$$

When (83) is satisfied, the subsequent update time $t_{i,k+1}$ is generated.

Remark 3.4. By selecting appropriate parameters γ_i and ε_i, the number of triggers generated by the ETC mechanism can be adjusted. As the parameter values increase, the frequency of triggering events decreases; conversely, smaller parameter values lead to an increased number of triggers. In particular, when both γ_i and ε_i are equal to 0, it becomes time-triggered.

From (80) to (83), we have

$$v_i(t) = (1+\lambda_{i1}(t)\gamma_i)u_i(t) + \lambda_{i2}(t)\varepsilon_i, \tag{84}$$

where $\lambda_{i1}(t)$ and $\lambda_{i2}(t)$ satisfy $|\lambda_{i1}(t)|\le 1$ and $|\lambda_{i2}(t)|\le 1$, respectively.

Then,

$$u_i(t) = \frac{v_i(t) - \lambda_{i2}(t)\varepsilon_i}{1+\lambda_{i1}(t)\gamma_i}. \tag{85}$$

4. Stability Analysis

In this section, we present our main results and conduct stability analysis.

Theorem 4.1. *Consider nonlinear switched MASs* (1) *with sensor faults* (2) *under Assumptions* 1–3, *where the initial states of the system satisfy the state constraints, and* $\hat{\varpi}_i(0) > 0$ *for all i. Based on the state observer (4), with the effect of the event-triggered controller (80), trigger condition (83), and associated virtual controllers (25), (46), (62), (66), (78), adaptive laws (26), (27), (47), (63), (67), (79), it is guaranteed that all signals of the closed-loop system are uniformly bounded. In addition, it ensures the achievement of the following control objectives.*

(i) *Observer error* $\tilde{x}_{iq}$, *error signal* z_{iq}, *consensus tracking error* $\bar{y}_i$, *adaptive parameter errors* $\tilde{\theta}_{iq}$ *and* $\tilde{\varpi}_i$ *are bounded and satisfy*

$$|\tilde{x}_{iq}| \le \sqrt{\bar{V}_n/\lambda_{\min}(P_i)}, \tag{86}$$

$$|z_{iq}| \le \tau_{iq}\sqrt{1-e^{-2\bar{V}_n}}, \tag{87}$$

$$\begin{aligned}|\bar{y}_i| \le & \sqrt{\bar{V}_n/\lambda_{\min}(P_i)} \\ & + \|(\mathcal{L}+\mathcal{B})^{-1}\|_\infty\bar{\tau}_1\sqrt{1-e^{-2\bar{V}_n}}, \end{aligned} \tag{88}$$

$$|\tilde{\theta}_{iq}| \leq \sqrt{2\eta_{iq}\bar{V}_n} \tag{89}$$

and

$$|\tilde{\varpi}_i| \leq (3w_i\bar{V}_n)^{\frac{1}{3}}, \tag{90}$$

where $q = 1, 2, \ldots, n,$ $i = 1, 2, \ldots, N$ *and* $\bar{V}_n = V_n(0) + \frac{M_n^*}{\beta_n}$*, the definition of* M_n^* *and* β_n *will be given in the course of the proof.*

(ii) *All system states always satisfy the state constraints, that is,* $|x_{iq}| < \tau_{c_{iq}}$*.*

(iii) *Zeno behavior does not occur.*

Proof. Since $\frac{1+\gamma_i}{1+\lambda_{i1}\gamma_i} \geq 1$, and $|\frac{\lambda_{i2}\varepsilon_i}{1+\lambda_{i1}\gamma_i}| \leq \frac{\varepsilon_i}{1-\gamma_i}$, then, according to (84), (85) and Lemma 2.8, we have

$$\begin{aligned}
\frac{z_{in}}{\tau_{in}^2 - z_{in}^2}u_i &\leq -\frac{z_{in}\alpha_{in}}{\tau_{in}^2 - z_{in}^2}\tanh\left(\frac{1}{\delta_i}\frac{z_{in}\alpha_{in}}{\tau_{in}^2 - z_{in}^2}\right) \\
&\quad - \frac{1}{1-\gamma_i}\frac{z_{in}\varepsilon_i}{\tau_{in}^2 - z_{in}^2}\tanh\left(\frac{1}{\delta_i(1-\gamma_i)}\frac{z_{in}\varepsilon_i}{\tau_{in}^2 - z_{in}^2}\right) \\
&\quad + \frac{1}{1-\gamma_i}\left|\frac{z_{in}\varepsilon_i}{\tau_{in}^2 - z_{in}^2}\right| \\
&\leq -\frac{z_{in}\alpha_{in}}{\tau_{in}^2 - z_{in}^2} + 0.557\delta_i.
\end{aligned} \tag{91}$$

Substituting (91) into (77), one has

$$\begin{aligned}
\dot{V}_n \leq& \sum_{i=1}^{N}\Bigg\{-\left(\varrho_i - 4\lambda_{\max}^2(P_i) - \frac{n}{2}\right)\|\tilde{x}_i\|^2 - \sum_{s=1}^{n-1}k_{is}\frac{z_{is}^2}{\tau_{is}^2 - z_{is}^2} \\
&+ \sum_{s=1}^{n-1}\frac{\eta_{is}^*}{\eta_{is}}\tilde{\theta}_{is}\hat{\theta}_{is} + \frac{w_i^*}{w_i}\varpi_i{}^2\varpi_i\mathrm{sign}(\tilde{\varpi}_i) \\
&- \frac{z_{in}\alpha_{in}}{\tau_{in}^2 - z_{in}^2} + \frac{z_{in}^2}{2(\tau_{in}^2 - z_{in}^2)^2} \\
&+ r_{in}\frac{z_{in}^2}{(\tau_{in}^2 - z_{in}^2)^2}\theta_{in} - \frac{1}{\eta_{in}}\tilde{\theta}_{in}\dot{\hat{\theta}}_{in} + M_{in} + 0.557\delta_i \\
\leq& \sum_{i=1}^{N}\Bigg\{-\left(\varrho_i - 4\lambda_{\max}^2(P_i) - \frac{n}{2}\right)\|\tilde{x}_i\|^2 - \sum_{s=1}^{n}k_{is}\frac{z_{is}^2}{\tau_{is}^2 - z_{is}^2} \\
&+ \sum_{s=1}^{n}\frac{\eta_{is}^*}{\eta_{is}}\tilde{\theta}_{is}\hat{\theta}_{is} + \frac{w_i^*}{w_i}\varpi_i{}^2\varpi_i\mathrm{sign}(\tilde{\varpi}_i) + \tilde{M}_{in}\Bigg\},
\end{aligned} \tag{92}$$

where $\tilde{M}_{in} = M_{in} + 0.557\delta_i$.

In addition,

$$\begin{aligned}
\tilde{\varpi}_i{}^2\hat{\varpi}_i\mathrm{sign}(\tilde{\varpi}_i) &= \tilde{\varpi}_i^2\hat{\varpi}_i\frac{|\tilde{\varpi}_i|}{\tilde{\varpi}_i} \\
&\leq |\tilde{\varpi}_i|^2\varpi_i - |\tilde{\varpi}_i|^3 \\
&\leq \frac{2}{3}|\tilde{\varpi}_i|^3 + \frac{1}{3}\varpi_i^3 - |\tilde{\varpi}_i|^3 \\
&= -\frac{1}{3}|\tilde{\varpi}_i|^3 + \frac{1}{3}\varpi_i^3
\end{aligned} \tag{93}$$

and

$$\begin{aligned}
\tilde{\theta}_{is}\hat{\theta}_{is} &= -\tilde{\theta}_{is}^2 + \tilde{\theta}_{is}\theta_{is} \\
&\leq -\tilde{\theta}_{is}^2 + \frac{1}{2}\tilde{\theta}_{is}^2 + \frac{1}{2}\theta_{is}^2 \\
&= -\frac{1}{2}\tilde{\theta}_{is}^2 + \frac{1}{2}\theta_{is}^2.
\end{aligned} \tag{94}$$

Substituting (93) and (94) into (92), one has

$$\begin{aligned}
\dot{V}_n \leq& \sum_{i=1}^{N}\Bigg\{-\left(\varrho_i - 4\lambda_{\max}^2(P_i) - \frac{n}{2}\right)\|\tilde{x}_i\|^2 - \sum_{s=1}^{n}k_{is}\frac{z_{is}^2}{\tau_{is}^2 - z_{is}^2} \\
&- \sum_{s=1}^{n}\frac{\eta_{is}^*}{\eta_{is}}\tilde{\theta}_{is}^2 - \frac{1}{3}\frac{w_i^*}{w_i}|\varpi_i|^3 + M_{in}^*\Bigg\},
\end{aligned} \tag{95}$$

where $M_{in}^* = \tilde{M}_{in} + \sum_{s=1}^{n}\frac{\eta_{is}^*}{\eta_{is}}\theta_{is}^2 + \frac{1}{3}\varpi_i^3$.

According to Lemma 2.10, one gets

$$-\frac{z_{is}^2}{\tau_{is}^2 - z_{is}^2} < -\log\frac{\tau_{is}^2}{\tau_{is}^2 - z_{is}^2}, \tag{96}$$

then inserting (96) into (95), one has

$$\begin{aligned}
\dot{V}_n \leq& \sum_{i=1}^{N}\Bigg\{-\left(\varrho_i - 4\lambda_{\max}^2(P_i) - \frac{n}{2}\right)\|\tilde{x}_i\|^2 - \sum_{s=1}^{n}k_{is}\log\frac{\tau_{is}^2}{\tau_{is}^2 - z_{is}^2} \\
&- \sum_{s=1}^{n}\frac{\eta_{is}^*}{\eta_{is}}\tilde{\theta}_{is}^2 - \frac{1}{3}\frac{w_i^*}{w_i}|\varpi_i|^3 + M_{in}^*\Bigg\} \\
\leq& -\beta_nV_n + M_n^*,
\end{aligned} \tag{97}$$

where

$$\begin{aligned}
\beta_n = \min\Bigg\{&\frac{\varrho_i - 3\lambda_{\max}(P_i) - \frac{n}{2}}{\lambda_{\max}(P_i)}, 2k_{i1}, 2k_{i2}, \ldots, 2k_{in}, \\
&\eta_{i1}^*, \eta_{i2}^*, \ldots, \eta_{in}^*, w^*\Bigg\},
\end{aligned}$$

and $M_n^* = \sum_{i=1}^{N}M_{in}^*$.

Then, we may come to the conclusion that the closed-loop systems are uniformly bounded.

(i) From (97), by and applying Comparison principle, we have

$$0 \leq V_n \leq \left(V_n(0) - \frac{M_n^*}{\beta_n}\right)e^{-\beta_nt} + \frac{M_n^*}{\beta_n} \leq \bar{V}_n. \tag{98}$$

From the definition of V_n, one has

$$\lambda_{\min}(P_i)|\tilde{x}_{iq}|^2 \leq \tilde{x}_i^TP_i\tilde{x}_i \leq V_n \leq \bar{V}_n, \tag{99}$$

then,

$$|\tilde{x}_{iq}| \leq \sqrt{\bar{V}_n/\lambda_{\min}(P_i)}. \tag{100}$$

Similarly,

$$\frac{1}{2}\log\frac{\tau_{iq}^2}{\tau_{iq}^2 - z_{iq}^2} \le V_n \le \bar{V}_n, \tag{101}$$

then one gets

$$|z_{iq}| \le \tau_{iq}\sqrt{1 - e^{-2\bar{V}_n}} \le \tau_{iq}. \tag{102}$$

From (17), one has

$$\begin{aligned}|\bar{y}_i| &= |y_i - y_r| = |y_i - \hat{y}_i + \hat{y}_i - y_r| \\ &\le |y_i - \hat{y}_i| + |\hat{y}_i - y_r| \\ &\le |\tilde{x}_{i1}| + \|\hat{y} - 1_N y_r\|_\infty \\ &\le \sqrt{\bar{V}_n/\lambda_{\min}(P_i)} + \|(\mathcal{L}+\mathcal{B})^{-1}z_1\|_\infty \\ &\le \sqrt{\bar{V}_n/\lambda_{\min}(P_i)} + \|(\mathcal{L}+\mathcal{B})^{-1}\|_\infty \bar{\tau}_1\sqrt{1 - e^{-2\bar{V}_n}},\end{aligned} \tag{103}$$

where $\bar{\tau}_1 = \max_{i=1,2,\ldots,N}\{\tau_{i1}\}$.

From the definition of V_n, one has

$$\frac{1}{2\eta_{iq}}\tilde{\theta}_{iq}^2 \le V_n \le \bar{V}_n, \tag{104}$$

then we have

$$|\tilde{\theta}_{iq}| \le \sqrt{2\eta_{iq}\bar{V}_n}. \tag{105}$$

Similarly, we can get

$$|\tilde{\varpi}_i| \le (3w_i\bar{V}_n)^{\frac{1}{3}}. \tag{106}$$

(ii) According to Assumption 3, y_r is bounded, that is, there exists a positive constant $\bar{y}_r$ such that $|y_r| \le \bar{y}_r$. Since $|x_{i1}| = |y_i| = |\bar{y}_i + y_r| \le |\bar{y}_i| + \bar{y}_r$, combined with the (103), and selecting the constraint function τ_{i1} satisfying

$$\tau_{i1} < \frac{\tau_{c_{i1}} - \sqrt{\bar{V}_n/\lambda_{\min}(P_i)} - \bar{y}_r}{\|(\mathcal{L}+\mathcal{B})^{-1}\|_\infty\sqrt{1 - e^{-2\bar{V}_n}}}, \tag{107}$$

then, one gets that $|x_{i1}| < \tau_{c_{i1}}$.

Note that $|x_{iq}| = |z_{iq} + \alpha_{q-1}| \le |z_{iq}| + |\alpha_{i,q-1}|$, $q = 2,\ldots,n$. Since the virtual controller $\alpha_{i,q-1}$ is continuous in some compact set, thus there exists a positive constant $\bar{\alpha}_{i,q-1}$ such that $|\alpha_{i,q-1}| \le \bar{\alpha}_{i,q-1}$. It follows from the boundedness of $\alpha_{i,q-1}$ and z_{iq} that x_{iq} is bounded. Choose constraint function τ_{iq} satisfying

$$\tau_{iq} < \frac{\tau_{c_{iq}} - \bar{\alpha}_{i,q-1}}{\sqrt{1 - e^{-2\bar{V}_n}}}, \tag{108}$$

then, one has $|x_{iq}| < \tau_{c_{iq}}$.

(iii) By the definition of $e_i(t)$, for $\forall t \in [t_{ik}, t_{i,k+1})$, we have

$$\frac{d}{dt}|e_i(t)| = \frac{d}{dt}\sqrt{e_i(t)e_i(t)} = |\dot{e}_i(t)| = |\dot{v}_i(t)|. \tag{109}$$

According to (81), $\dot{v}_i(t)$ is continuous in some compact set, thus, there exists a positive constant $\bar{v}_i$ such that $|\dot{v}_i(t)| \le \bar{v}_i$.

Integrate the both ends of (109) from t_{ik} to $t_{i,k+1}$, we have

$$\begin{aligned}&\int_{t_{ik}}^{t_{i,k+1}} \frac{d}{dt}|\dot{e}_i(t)|dx \\ &\quad = |e_i(t_{i,k+1})| - |e_i(t_{ik})| \\ &\quad \le \bar{v}_i(t_{i,k+1} - t_{ik}).\end{aligned} \tag{110}$$

Noticing that $e_i(t_{ik}) = 0$ and $\lim_{t\to t_{i,k+1}}|e_i(t)| = \gamma_i|u_i(t_{i,k+1})| + \epsilon_i$, one gets

$$t_{i,k+1} - t_{ik} \ge \frac{\gamma_i|u_i(t_{i,k+1})| + \varepsilon_i}{\bar{v}_i} > 0. \tag{111}$$

As a result, the Zeno behavior can be excluded. □

5. Simulation

In this section, a practical application example is presented to verify the validity of our theoretical results.

Considers the consensus tracking problem for four single-link manipulators to track the leader signal $y_r = 0.5\sin(t) + \cos(3t)$.

The mathematical model of a single-link manipulator can be expressed as follows:

$$a_i^\sigma\dot{v}_i + b_i^\sigma\ddot{v}_i + c_i^\sigma\sin(v_i) = u_i + \pi_i^\sigma, \quad i = 1,2,3,4, \tag{112}$$

where v_i represents the angle of the rigid link, $\dot{v}_i$ is the angular velocity, $\ddot{v}_i$ is the acceleration of the link, and π_i^σ is torque disturbance. The interactions of five agents are shown in Fig. 1. The change of the switching index $\sigma(t)$ is shown in Fig. 2. When $\sigma = 1$, $a_i^\sigma = b_i^\sigma = 1$, $c_i^\sigma = 1.5$ and $\pi_i^\sigma = 0.3\cos(2t)$; when $\sigma = 2$, $a_i^\sigma = 1, b_i^\sigma = 0.8, c_i^\sigma = 1$ and $\pi_i^\sigma = 0.2\sin(5t)$.

Let $x_{i1} = v_i$ and $x_{i2} = \dot{v}_i$. For $\sigma = 1$, system (112) can be written as

$$\begin{cases}\dot{x}_{i1} = x_{i2}, \\ \dot{x}_{i2} = u_i - x_{i2} - 1.5\sin(x_{i1}) + 0.3\cos(2t), \\ y_i = x_{i1}.\end{cases} \tag{113}$$

For $\sigma = 2$, it can be written as

$$\begin{cases}\dot{x}_{i1} = x_{i2}, \\ \dot{x}_{i2} = u_i - 0.8x_{i2} - \sin(x_{i1}) + 0.2\sin(5t), \\ y_i = x_{i1}.\end{cases} \tag{114}$$

Set the sensor fault time t_i^F, $i = 1,2,3,4$, to $t_1^F = 4.3s$, $t_2^F = 6.6s$, $t_3^F = 18.4s$ and $t_4^F = 23s$, respectively.

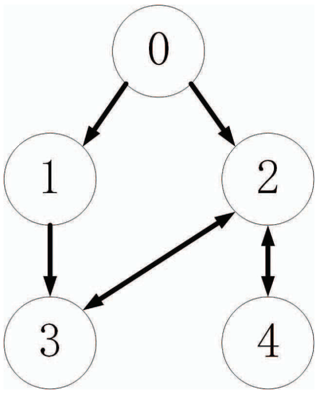

Fig. 1. Directed interaction graph.

The actual outputs setting of the MASs under sensor faults are as follows:

$$y_1^F = \begin{cases} x_{11}, & t \le 4.3s, \\ 0.72x_{11}, & t > 4.3s, \end{cases} \tag{115}$$

$$y_2^F = \begin{cases} x_{21}, & t \le 6.6s, \\ 0.9x_{21}, & t > 6.6s, \end{cases} \tag{116}$$

$$y_3^F = \begin{cases} x_{31}, & t \le 18.4s, \\ 0.78x_{21}, & t > 18.4s, \end{cases} \tag{117}$$

and

$$y_4^F = \begin{cases} x_{41}, & t \le 23s, \\ 0.88x_{21}, & t > 23s. \end{cases} \tag{118}$$

The state constraint functions are given as $\tau_{c_{11}} = 2e^{-t} + 1.65$, $\tau_{c_{12}} = 5e^{-t} + 12$, $\tau_{c_{21}} = 2e^{-t} + 1.65$, $\tau_{c_{22}} = 5e^{-t} + 12$, $\tau_{c_{31}} = 2e^{-t} + 1.65$, $\tau_{c_{32}} = 5e^{-t} + 12$, $\tau_{c_{41}} = 2e^{-t} + 1.65$ and $\tau_{c_{42}} = 3e^{-t} + 12$, where $\tau_{c_{i1}}$ and $\tau_{c_{i2}}$, $i = 1, 2, 3, 4$, are the constraint functions of states x_{i1} and x_{i2}, respectively.

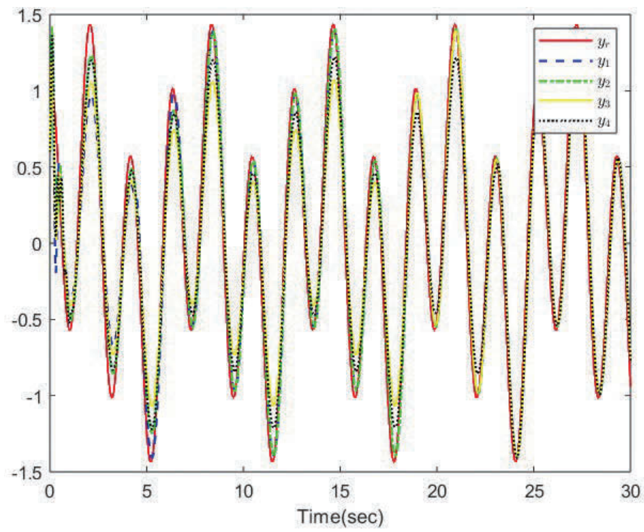

Fig. 3. The trajectories of y_1, y_2, y_3, y_4 and y_r.

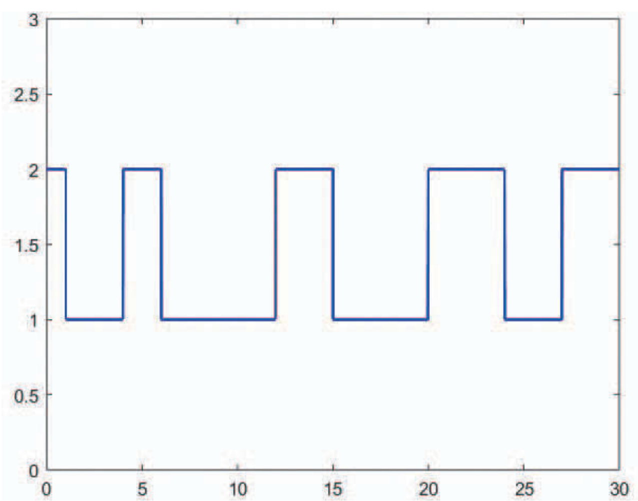

Fig. 2. Switching signal $\sigma(t)$.

The initial values of the state are set to $x_{11}(0) = 0.6$, $x_{12}(0) = -0.5$, $x_{21}(0) = 0.2$, $x_{22}(0) = 0.8$, $x_{31}(0) = 0.23$, $x_{32}(0) = 0.78$, $x_{41}(0) = 0.19$ and $x_{42}(0) = 0.82$. The initial values of $\hat{\varpi}_i$, $i = 1, 2, 3, 4$, are set to 0. The rest of the initial values are set to 1.

The parameters are selected as $l_{11} = l_{21} = l_{31} = l_{41} = 3$, $l_{12} = l_{22} = l_{32} = l_{42} = 60$. $k_{11} = 20$, $k_{21} = 40$, $k_{31} = 20$, $k_{41} = 20$, $r_{11} = 10$, $r_{21} = 10$, $r_{31} = 5$, $r_{41} = 5$, $\eta_{11} = \eta_{21} = 8, \eta_{31} = \eta_{41} = 16$, $\eta_{11}^* = \eta_{21}^* = \eta_{31}^* = \eta_{41}^* = 10$, $k_{12} = 40$, $k_{22} = 40$, $k_{32} = 20$, $k_{42} = 20$, $r_{12} = 10$, $r_{22} = 10$, $r_{32} = 5, r_{42} = 5, \eta_{12} = \eta_{22} = 8, \eta_{32} = \eta_{42} = 16$, $\eta_{12}^* = \eta_{22}^* = \eta_{32}^* = \eta_{42}^* = 10, w_1 = w_2 = w_3 = w_4 = 8$, $w_1^* = w_2^* = w_3^* = w_4^* = 1$, $\gamma_1 = \gamma_2 = \gamma_3 = \gamma_4 = 0.8$ and $\varepsilon_1 = \varepsilon_2 = \varepsilon_3 = \varepsilon_4 = 0.79$.

After 30 s of simulation time, the simulation results are shown in Figs. 3–10. Figure 3 shows the trajectories of the output signal y_1, y_2, y_3, y_4 and the leader signal y_r. It can be observed from Fig. 3 that the output signals of the followers converge to the leader signal with small errors. Figures 4 and 5 showcase the trajectories of system states x_{i1}, x_{i2} and their estimations $\hat{x}_{i1}$, $\hat{x}_{i2}$, which are tightly controlled within predefined boundaries $\tau_{c_{i1}}$ and $\tau_{c_{i2}}$. Figures 6 and 7 depict the trajectories of errors z_{i1} and z_{i2}, which remain within the predefined time-varying boundaries τ_{i1} and τ_{i2}. The black dots in the figures mark the moments of sensor faults. Figure 8 exhibits the curves of the ETC signals u_i. Compared with the time-triggered mechanisms, this strategy significantly reduces the update frequency of the controller, saves the system computing resources, and improves the system efficiency. Figure 9 shows the trigger time t_{ik} and the inter-event time $t_{i,k+1} - t_{ik}$, which indicate the absence of the

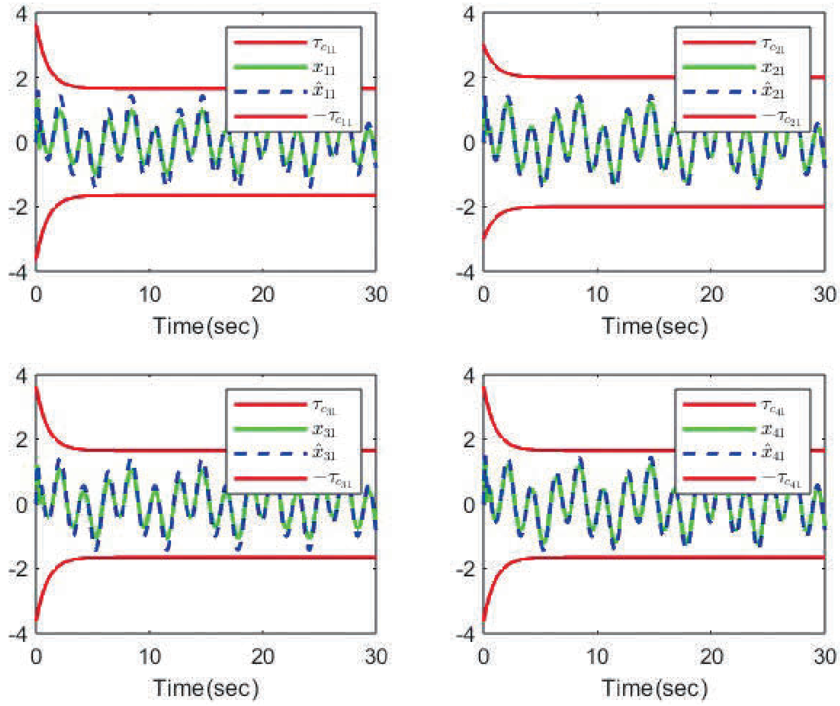

Fig. 4. Trajectories of x_{i1} and $\hat{x}_{i1}$, $i = 1, 2, 3, 4$, with constraints.

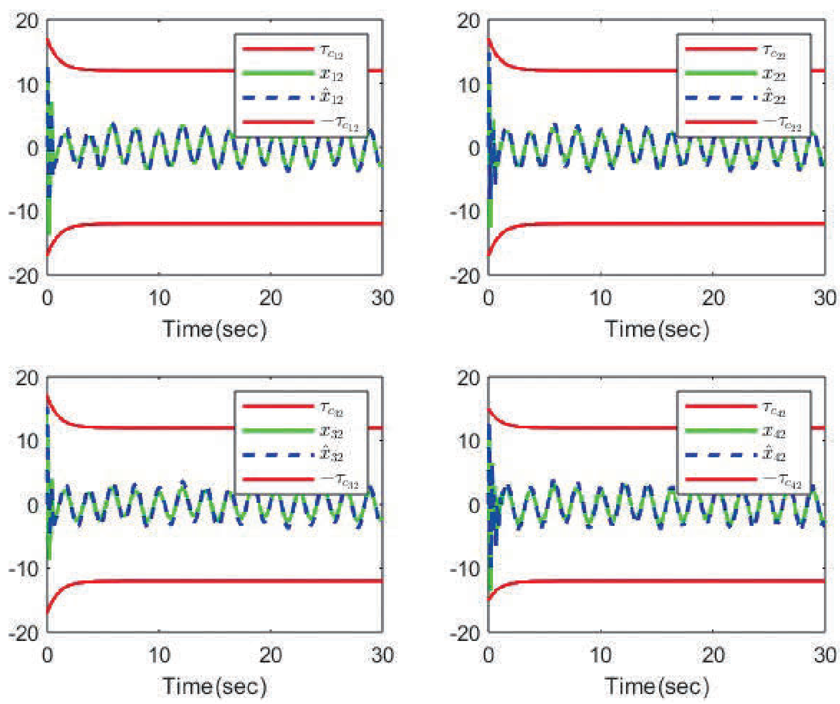

Fig. 5. Trajectories of x_{i2} and $\hat{x}_{i2}$, $i = 1, 2, 3, 4$, with constraints.

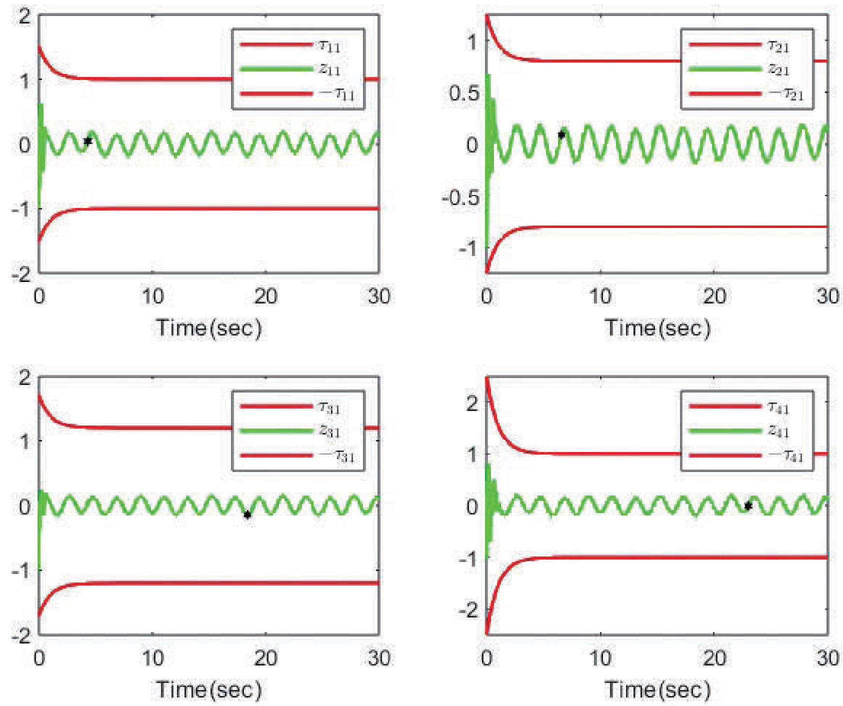

Fig. 6. Trajectories of the consensus errors z_{i1}, $i = 1, 2, 3, 4$.

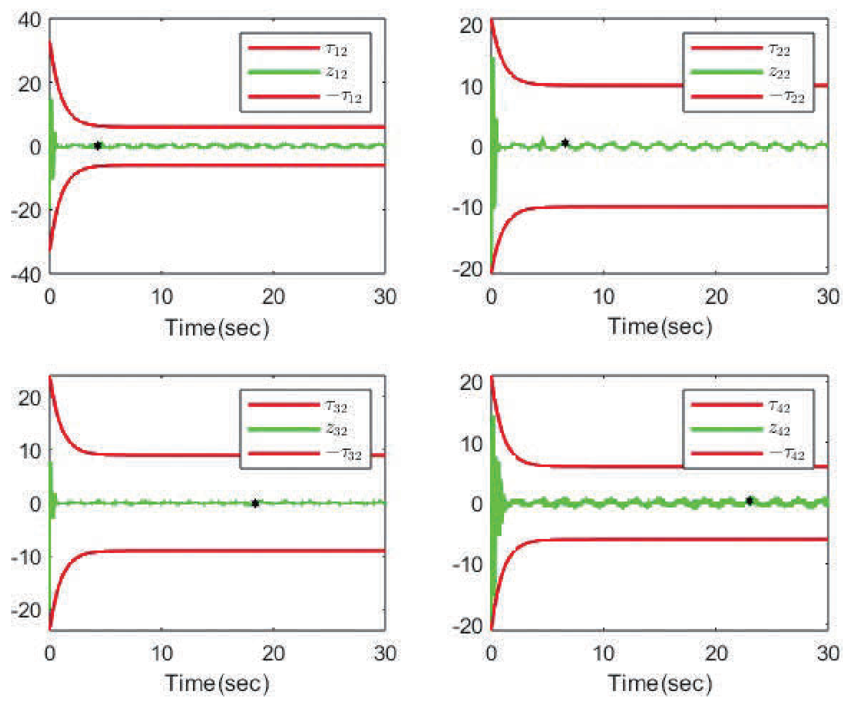

Fig. 7. Trajectories of the consensus errors z_{i2}, $i = 1, 2, 3, 4$.

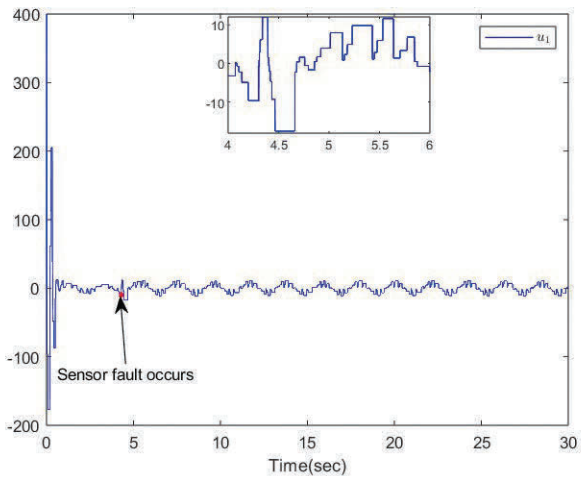

(a) u_1

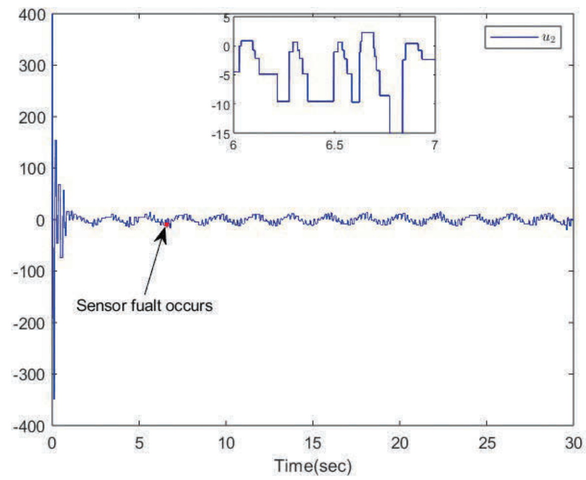

(b) u_2

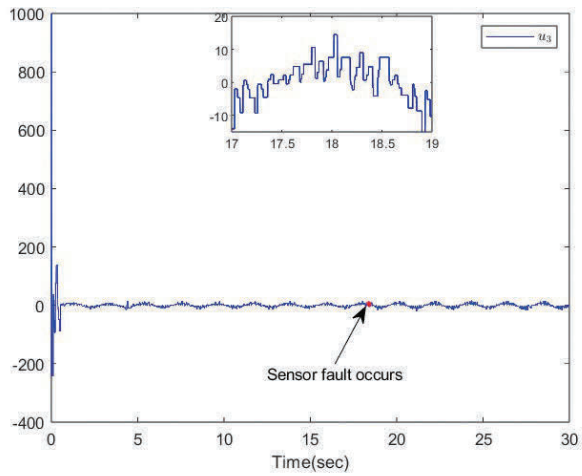

(c) u_2

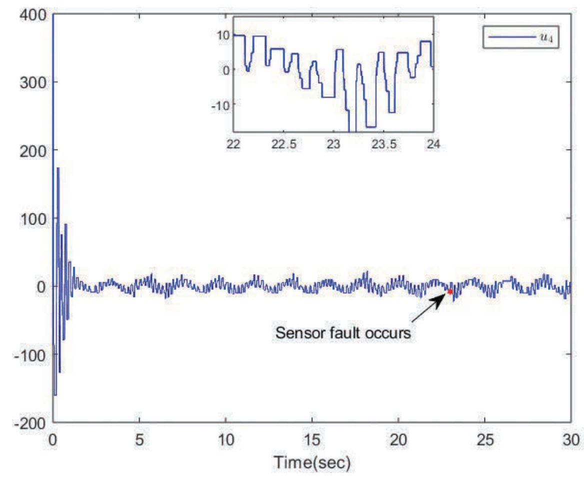

(d) u_4

Fig. 8. Curve of the event-triggered controller u_1, u_2, u_3, u_4.

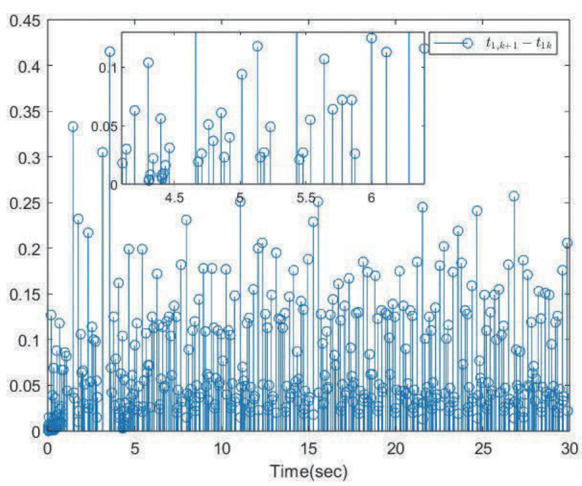

(a) u_1

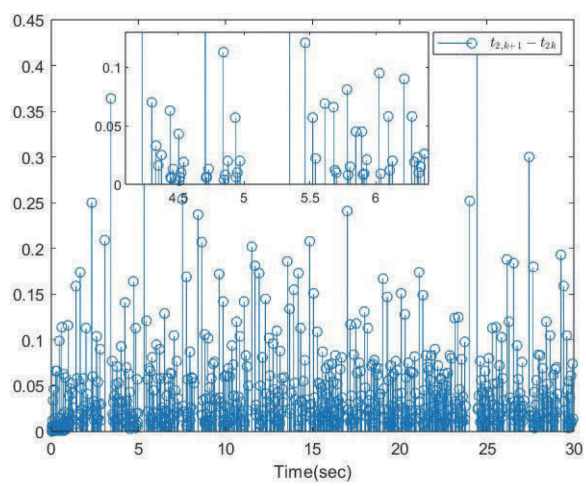

(b) u_2

Fig. 9. The inter-event time $t_{i,k+1} - t_{ik}$, $i = 1, 2, 3, 4$.

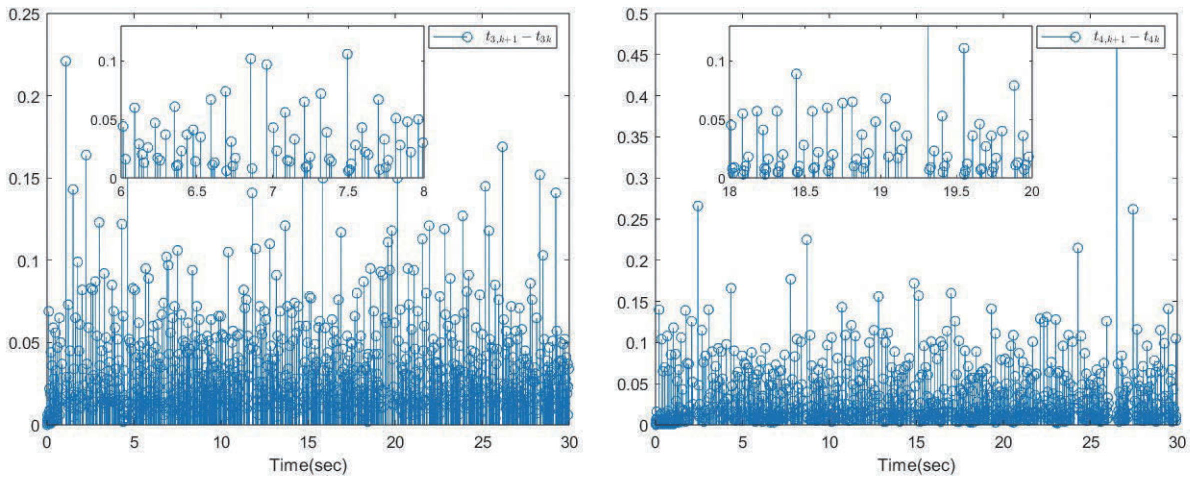

(c) u_2 (d) u_4

Fig. 9. (*Continued*)

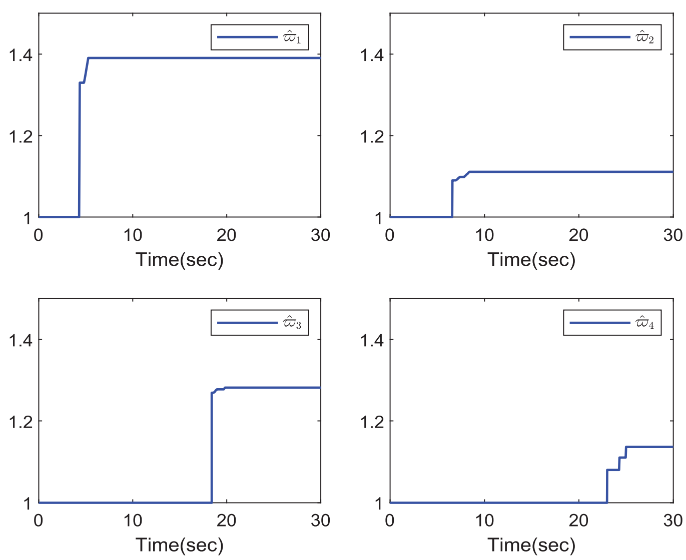

Fig. 10. The trajectory of $\hat{\varpi}_i, i = 1, 2, 3, 4$.

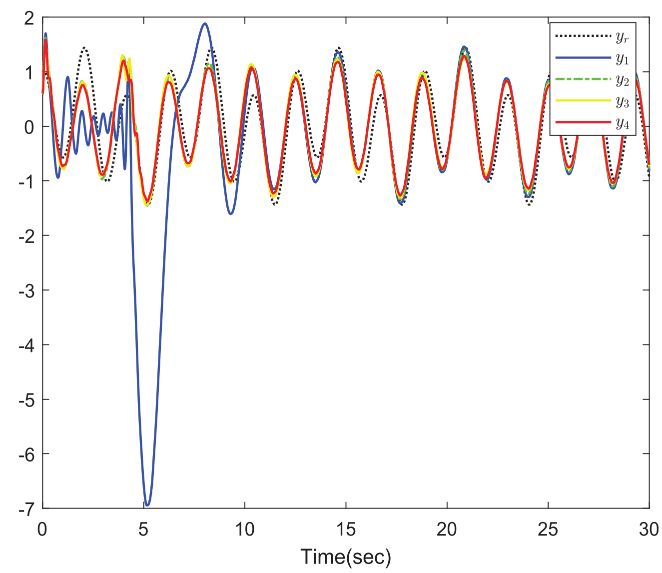

Fig. 11. The trajectories of y_1, y_2, y_3, y_4 and y_r with $\iota_1 = 0.01$.

Zeno phenomenon in the system. Figure 10 displays the trajectories of estimation parameters $\hat{\varpi}_i$. The designed adaptive fault compensation coefficient successfully compensates for the system deviation caused by sensor faults, thus ensuring the stability and reliability of the system when a sensor fault occurs.

Moreover, for the extreme cases such as $\iota_1 = 0.01$, the system response curve shown in Fig. 11 can be obtained by selecting appropriate parameters. It can be observed from Fig. 11 that the output signals of the following agents can still gradually synchronize with the leader signal after experiencing large fluctuations.

6. Conclusion

In this paper, the problem of event-triggered fuzzy control for a class of switched nonlinear MASs with sensor faults is studied. Because the states of the system are unmeasurable, a state observer is designed based on output feedback to estimate the unmeasurable states. For unknown sensor faults, the adaptive compensation coefficients of sensor faults are designed to ensure the stable operation of the system. By selecting the appropriate barrier Lyapunov function, the state constraint problem of the system is dealt with. FLS is used to approximate the unknown nonlinear dynamics in the system, and the unknown parameters are adaptively adjusted. Through stability analysis, the proposed algorithm can ensure that the follower agents track the leader's signal and make the closed-loop system uniformly bounded. For the proposed ETC mechanism, it is proved that it will not cause Zeno behavior, thus ensuring the smooth operation of the system. Finally, the effectiveness of the algorithm is verified by computer simulation.

ORCID

Zhen Duan https://orcid.org/0009-0005-3733-8309
Hui Yu https://orcid.org/0000-0001-5862-6733

References

[1] N. R. Gans and J. G. Rogers, Cooperative multirobot systems for military applications, *Curr. Robot. Rep.* **2**(1) (2021) 105–111.
[2] K. Antoniadou-Plytaria, I. Kouveliotis-Lysikatos, P. Georgilakis and N. D. Hatziargyriou, Distributed and decentralized voltage control of smart distribution networks: Models, methods and future research, *IEEE Trans. Smart Grid* **8**(6) (2017) 2999–3008.
[3] F. Yang, Z. Liu and Y. Zhao, Event-triggered neural adaptive tracking control for output constrained nonlinear multi-agent systems with unmodeled dynamics and unknown signs, *Syst. Control Lett.* **186** (2024) 105757.
[4] Y. Rizk, M. Awad and E. W. Tunstel, Cooperative heterogeneous multi-robot systems: A survey, *ACM Comput. Surv.* **52**(2) (2019) 1–31.
[5] W. Wang, J. Long, C. Wen and J. Huang, Recent advances in distributed adaptive consensus control of uncertain nonlinear multi-agent systems, *J. Control Decis.* **7**(1) (2020) 44–63.
[6] C. Gao, X. He, H. Dong, H. Liu and G. Lyu, A survey on fault-tolerant consensus control of multi-agent systems: Trends, methodologies and prospects, *Int. J. Syst. Sci.* **53**(13) (2022) 2800–2813.
[7] Z. Gong and F. Yang, Secure tracking control via fixed-time convergent reinforcement learning for a UAV CPS, *IEEE/CAA J. Autom. Sinica* **11**(7) (2024) 1699–1701.
[8] Z. Ma and S. Sun, Research on vehicle-to-road collaboration and end-to-end collaboration for multimedia services in the internet of vehicles, *IEEE Access* **10** (2021) 18146–18155.
[9] W. Zou, P. Shi, Z. Xiang and Y. Shi, Finite-time consensus of second-order switched nonlinear multi-agent systems, *IEEE Trans. Neural Netw. Learn. Syst.* **31**(5) (2019) 1757–1762.
[10] W. Zhang, D. W. C. Ho, Y. Tang and Y. Liu, Quasi-consensus of heterogeneous-switched nonlinear multiagent systems, *IEEE Trans. Cybern.* **50**(7) (2019) 3136–3146.
[11] W. Zou, C. K. Ahn and Z. Xiang, Fuzzy-approximation-based distributed fault-tolerant consensus for heterogeneous switched nonlinear multiagent systems, *IEEE Trans. Fuzzy Syst.* **29**(10) (2020) 2916–2925.
[12] S. Li, W. Zou, J. Guo and Z. Xiang, Consensus of switched nonlinear multiagent systems subject to cyber attacks, *IEEE Syst. J.* **16**(3) (2021) 4423–4432.
[13] L. Shang and M. Cai, Adaptive practical fast finite-time consensus protocols for high-order nonlinear multi-agent systems with full state constraints, *IEEE Access* **9** (2021) 81554–81563.
[14] G. Zhu, H. Li, X. Zhang, C. Wang, C.-Y. Su and J. Hu, Adaptive consensus quantized control for a class of high-order nonlinear multi-agent systems with input hysteresis and full state constraints, *IEEE/CAA J. Autom. Sinica* **9**(9) (2022) 1574–1589.
[15] C. Ke, C. Li and Q. Zhang, Distributed adaptive fault-tolerant consensus of nonlinear multi-agent systems via state-constraint impulsive protocols with time-delay, *IEEE Trans. Netw. Sci. Eng.* **7**(4) (2020) 3112–3121.
[16] J. Wang, Y. Yan, Z. Liu, C. L. P. Chen, C. Zhang and K. Chen, Finite-time consensus control for multi-agent systems with full-state constraints and actuator failures, *Neural Netw.* **157** (2023) 350–363.
[17] J. Shi, Cooperative control for nonlinear multi-agent systems based on event-triggered scheme, *IEEE Trans. Circuits Syst. II Express Briefs* **68**(6) (2020) 1977–1981.
[18] Y. Xu, T. Li, Y. Yang, Q. Shan, S. Tong and C. L. P. Chen, Anti-attack event-triggered control for nonlinear multi-agent systems with input quantization, *IEEE Trans. Neural Netw. Learn. Syst.* **34** (2022) 10105–10115.
[19] W. Zou, P. Shi, Z. Xiang and Y. Shi, Consensus tracking control of switched stochastic nonlinear multiagent systems via event-triggered strategy, *IEEE Trans. Neural Netw. Learn. Syst.* **31**(3) (2019) 1036–1045.
[20] J. Gao, J. Li, H. Pan, Z. Wu, X. Yin and H. Wang, Consensus via event-triggered strategy of nonlinear multi-agent systems with Markovian switching topologies, *ISA Trans.* **104** (2020) 122–129.
[21] W. Zou and Z. Xiang, Event-triggered leader–following consensus of non-linear multi-agent systems with switched dynamics, *IET Control Theory Appl.* **13**(9) (2019) 1222–1228.
[22] R. Hao, H. Wang and W. Zheng, Dynamic event-triggered adaptive command filtered control for nonlinear multi-agent systems with input saturation and disturbances, *ISA Trans.* **130** (2022) 104–120.
[23] H. Zhang, J. Zhang, Y. Cai, S. Sun and J. Sun, Leader-following consensus for a class of nonlinear multiagent systems under event-triggered and edge-event triggered mechanisms, *IEEE Trans. Cybern.* **52**(8) (2020) 7643–7654.
[24] M. Rehan, M. Tufail and S. Ahmed, Leaderless consensus control of nonlinear multi-agent systems under directed topologies subject to input saturation using adaptive event-triggered mechanism, *J. Franklin Inst.* **358**(12) (2021) 6217–6239.
[25] D. Yao, H. Li, R. Lu and Y. Shi, Distributed sliding-mode tracking control of second-order nonlinear multiagent systems: An event-triggered approach, *IEEE Trans. Cybern.* **50**(9) (2020) 3892–3902.
[26] Y. Li, F. Qu and S. Tong, Observer-based fuzzy adaptive finite-time containment control of nonlinear multiagent systems with input delay, *IEEE Trans. Cybern.* **51**(1) (2020) 126–137.
[27] H. Yang and D. Ye, Adaptive fuzzy nonsingular fixed-time control for nonstrict-feedback constrained nonlinear multiagent systems with input saturation, *IEEE Trans. Fuzzy Syst.* **29**(10) (2020) 3142–3153.
[28] Z. Liu, H. Huang, J. H. Park, J. Huang, X. Wang and M. Lv, Adaptive fuzzy control for unknown nonlinear multiagent systems with switching directed communication topologies, *IEEE Trans. Fuzzy Syst.* **31**(7) (2023) 2487–2494.
[29] C.-E. Ren, C. L. P. Chen, T. Du and Y. Guan, Fuzzy adaptive leader-following consensus control for nonlinear multi-agent systems with unknown control directions, *Int. J. Fuzzy Syst.* **21** (2019) 2066–2076.
[30] X. Fan, P. Bai, H. Li, X. Deng and M. Lv, Adaptive fuzzy finite-time tracking control of uncertain non-affine multi-agent systems with input quantization, *IEEE Access* **8** (2020) 187623–187633.
[31] W. Wang, H. Liang, Y. Pan and T. Li, Prescribed performance adaptive fuzzy containment control for nonlinear multiagent systems using disturbance observer, *IEEE Trans. Cybern.* **50**(9) (2020) 3879–3891.
[32] Y. Li, K. Li and S. Tong, An observer-based fuzzy adaptive consensus control method for nonlinear multiagent systems, *IEEE Trans. Fuzzy Syst.* **30**(11) (2022) 4667–4678.

[33] J. Zhang and Z. Xiang, Event-triggered adaptive neural network sensor failure compensation for switched interconnected nonlinear systems with unknown control coefficients, *IEEE Trans. Neural Netw. Learn. Syst.* **33**(10) (2021) 5241–5252.
[34] Y. Ma, Z. Li, X. Xie and D. Yue, Adaptive consensus of uncertain switched nonlinear multi-agent systems under sensor deception attacks, *Chaos Solitons Fractals* **175** (2023) 113936.
[35] X. Wang, Y. Zhou, T. Huang and P. Chakrabarti, Event-triggered adaptive fault-tolerant control for a class of nonlinear multiagent systems with sensor and actuator faults, *IEEE Trans. Circuits Syst. I Regul. Pap.* **69**(10) (2022) 4203–4214.
[36] L. Cao, H. Li, G. Dong and R. Lu, Event-triggered control for multiagent systems with sensor faults and input saturation, *IEEE Trans. Syst. Man Cybern. Syst.* **51**(6) (2019) 3855–3866.
[37] Y. Yu, J. Guo and Z. Xiang, Distributed fuzzy consensus control of uncertain nonlinear multiagent systems with actuator and sensor failures, *IEEE Syst. J.* **16**(3) (2021) 3480–3487.
[38] X. Chen and F. Hao, Observer-based event-triggered control for certain and uncertain linear systems, *IMA J. Math. Control Inf.* **30**(4) (2013) 527–542.
[39] W. Ren and R. W. Beard, Consensus seeking in multiagent systems under dynamically changing interaction topologies, *IEEE Trans. Autom. Control* **50**(5) (2005) 655–661.
[40] D. Zhai, L. An, J. Dong and Q. Zhang, Output feedback adaptive sensor failure compensation for a class of parametric strict feedback systems, *Automatica* **97** (2018) 48–57.
[41] X. Liu, D. Zhai, T. Li and Q. Zhang, Fuzzy-approximation adaptive fault-tolerant control for nonlinear pure-feedback systems with unknown control directions and sensor failures, *Fuzzy Sets Syst.* **356** (2019) 28–43.
[42] L.-X. Wang, *Adaptive Fuzzy Systems and Control: Design and Stability Analysis* (Prentice-Hall, 1994).
[43] B. Ren, P. P. San, S. S. Ge and T. H. Lee, Adaptive dynamic surface control for a class of strict-feedback nonlinear systems with unknown backlash-like hysteresis, in *2009 American Control Conf.* (IEEE, 2009), pp. 4482–4487.
[44] H. Deng and M. Krstic, Output-feedback stochastic nonlinear stabilization, *IEEE Trans. Autom. Control* **44**(2) (1999) 328–333.
[45] B. Ren, S. S. Ge, K. P. Tee and T. H. Lee, Adaptive neural control for output feedback nonlinear systems using a barrier Lyapunov function, *IEEE Trans. Neural Netw.* **21**(8) (2010) 1339–1345.
[46] T. Wu, Z. Yu and S. Li, Observer-based adaptive fuzzy quantized fault-tolerant control of nonstrict-feedback nonlinear systems with sensor fault, *IEEE Trans. Fuzzy Syst.* **31**(6) (2022) 1900–1911.
[47] K. B. Ngo, R. Mahony and Z.-P. Jiang, Integrator backstepping using barrier functions for systems with multiple state constraints, in *Proc. 44th IEEE Conf. Decision and Control* (IEEE, 2005), pp. 8306–8312.

Zhen Duan received his B.S. degree in Pharmaceutical Engineering from the Taishan Medical University, in 2013, and now he is a master degree candidate in Mathematics in China Three Gorges University. His research interests include complex dynamical network, consensus problem of multi-agent systems.

Hui Yu received his bachelor's degree in Mathematics from the Central China Normal University, Wuhan, China in 1991, his master's degree in System Analysis and Integration from the East China Normal University, Shanghai, China in 1999, and his Ph.D. degree in Control Theory and Control Engineering from the Huazhong University of Science and Technology, Wuhan, China in 2007. From 2011 to 2012, he was visiting the Centre of New Energy Systems, Department of Electrical, Electronics and Computer Engineering, University of Pretoria, South Africa. Since 1991, he has been with College of Science, China Three Gorges University, where he is currently a professor. His research interests include nonlinear control theory with applications to multi-agent systems and robots.